Chem. Rev. 1991, 91, 823–842

Ab Initio Molecular Orbital Studies of Catalytic Elementary Reactions and Catalytic Cycles of Transition-Metal Complexes

NOBUAKI KOGA* and KEIJI MOROKUMA*

Institute for Molecular Science, Myodaiji, Okazaki 444, Japan

Received March 4, 1991 (Revised Manuscript Received May 7, 1991)

Contents

I. Introduction

Chemical reaction catalyzed by transition-metal complex can be regarded as a sequence of elementary reactions such as olefin insertion, carbonyl insertion, oxidative addition, and reductive elimination.[1] These elementary steps have been studied with various theoretical methods such as the semiempirical and the ab initio molecular orbital (MO) method and the density functional theory.[2] In studies using the extended Hückel method,[3] symmetry arguments rather than energy arguments have been preferred, although discussion has been sometimes made on the basis of energy.[2a,4] The symmetry argument is useful, when a reaction is discussed very qualitatively.[2a] However, one often needs more quantitative information, when one wants to systematically examine electronic effects on the reactivity caused by transition metal, substituent, ligand, coordination number, and so forth. Semiempirical methods could not be used reliably for this purpose.

Through late 1970's and 1980's, the ab initio energy gradient method has been applied to varieties of organic reactions.[5] With the energy gradient, one can optimize the structure of a transition state (TS) as well as a reactant and a product. The geometry optimization has been found to be essential for reliable determination of the energy of reaction and the activation energy. The application of the energy gradient method to transition-metal complexes has been more difficult because of many electrons to be included in the calculation and many degrees of freedom to be optimized. However, in the last several years, we have seen substantial activities, supported by the advance in the ab initio MO method and code as well as in the speed of computers, in the theoretical study of elementary reactions and catalytic cycles.[2b] Catalytic cycles contain some fast elementary reactions, for which experimental determination of the structure of intermediates or the kinetics is not possible for each reaction. Ab initio MO calculations can provide such information, though in many cases, only for models of real reacting systems. In addition, the effect of changing a transition metal, a substituent, or a ligand on the reactivity can be relatively easily investigated. Such information should be an essential ingredient for controlling and designing a catalytic cycle.

It is the effective core potential (ECP) approximation that made the computation practical for heavy transition metal complexes.[6] The ECP, also called pseudo-

Nobuaki Koga was born in 1958. He received his B.Sc. and Ph.D. degrees from Kyoto University in 1979 and 1987, respectively. He joined Keiji Morokuma's group at the Institute for Molecular Science in 1983 and is presently a Research Associate. His research interests include quantum chemistry of organometallic as well as organic reactions.

Keiji Morokuma, Ph.D. from Kyoto University, did postdoctoral work at Columbia and Harvard and in 1967 joined the faculty of Department of Chemistry, University of Rochester, where he last served as Professor of Chemistry. In 1976 he moved back to Japan to join the newly formed Institute for Molecular Science as Professor of Theoretical Studies and has been Director of Department of Theoretical Studies and of Computer Center. His recent research interest has been focused on chemical reactivity, including potential surfaces and dynamics of excited gas phase molecules as well as organic and organometallic reactions.

0009-2665/91/0791-0823$09.50/0

TABLE I. Energy of Reaction (ΔE) and Activation Energy ($\Delta E^{\ddagger}$) (in kcal/mol) of Ethylene Insertion into an M–H Bond Calculated at the RHF Level (numbers in parentheses are at the MP2 level[a])

	$\Delta E^{\ddagger}$	ΔE	ref
reaction 1			
M = Ni	0.6	−31.5	11
M = Pd	8.0 (5.1)	−3.0 (3.0)	11
M = Pt	12.5	4.2	11
reaction 2	16.4 (18.6)	18.4 (25.5)	12
reaction 3	21.2 (23.4)–23.0	−11.7 to −13.5	13

[a] Calculated at the RHF optimized structures.

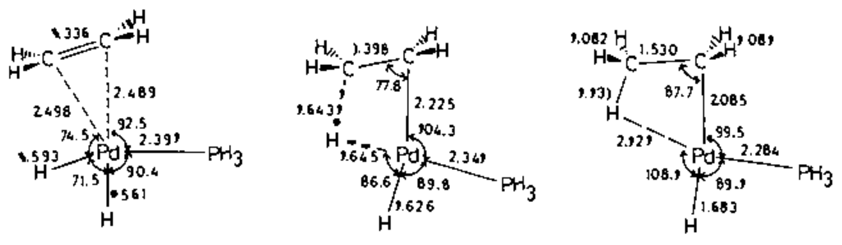

Figure 1. Structures (in angstroms and degrees), optimized at the RHF level, of reactant, 1, product, 2, and transition state for ethylene insertion/β-hydrogen elimination of the Pd complex.[11]

potential (PP) or model potential,[7] replaces the core electrons by the Coulomb and exchange potential due to core electrons acting on valence electrons. Therefore, by using ECP, the number of electrons in the calculation could be reduced with a small decrease in reliability. In addition, one can incorporate into ECP the relativistic effect, which is important in a heavy atom. The direct relativistic effect stabilizes and contracts s orbitals and, as a result, d orbitals become higher in energy and more diffuse (the indirect relativistic effect).[8] Consequently, the relativistic effect must be taken into account in the calculation of a complex of a heavy transition metal, especially the second and the third row transition metal. The ECP has been used in many studies as will be shown here.

In this article, we review ab initio MO studies of elementary reactions and catalytic cycles of transition-metal complexes. In earlier studies the energy gradient method has not been used but the structures were partially optimized by using only energy. Consequently, reactions studied have been limited to relatively small systems. However, since such studies have given some useful results, they are included here as well as the studies by the energy gradient method. Recently, energy gradient method with the density functional theory has been developed, with which several organometallic reactions has been studied.[9] They will be discussed in another article of this special issue.[10] The elementary reactions of insertion, nucleophilic addition to coordinated ligands, oxidative addition/reductive elimination, and metathesis will be discussed in section II and the catalytic cycles in section III. The section IV will be concluding remarks.

II. Elementary Reactions of Transition-Metal Complexes

A. Olefin Insertion

Olefin insertion into an M–H bond is an essential step for conversion of olefin to alkyl in a catalytic reaction and thus several model insertion reactions have been studied. By means of the ab initio MO method, Koga, Morokuma, and their co-workers have studied ethylene insertion of d^8 square-planar ethylene hydride complexes (reaction 1),[11] d^6 octahedral ethylene hydride complexes (reaction 2),[12] and d^8 trigonal-bipyramidal (TBP) ethylene hydride complexes (reaction 3).[13] They

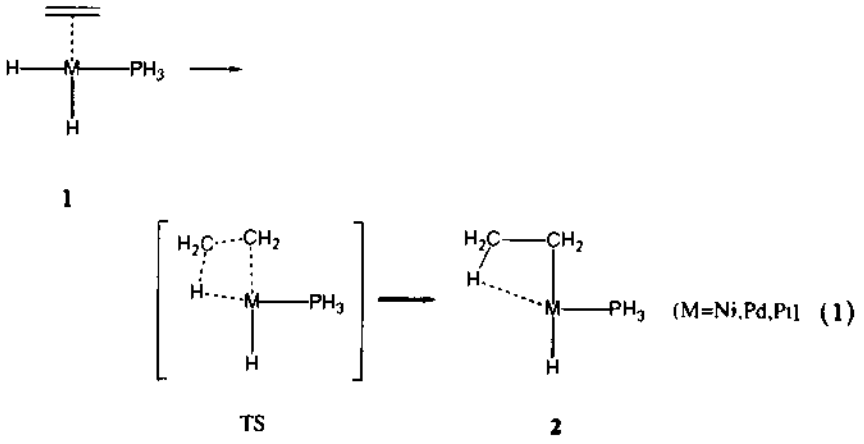

1 TS 2 (1)

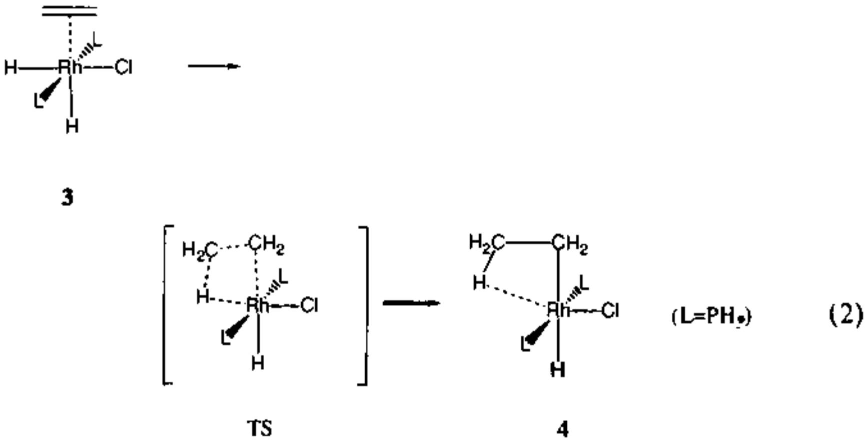

3 TS 4 (2)

$$\mathrm{Rh(H)(CO)_2(PH_3)(C_2H_4)}\ (5) \rightarrow \mathrm{Rh(CO)_2(PH_3)(C_2H_5)}\ (6) \quad (3)$$

have determined the structures of the transition states with the restricted Hartree–Fock and ECP (RHF-ECP) energy gradient method and took into account the electron correlation effect by the second-order Møller–Plesset perturbation theory (MP2).[14] The energetics is summarized in Table I. All the above olefin insertions have been found to pass through four-centered TSs. The optimized structures of the reactant, the product, and the TS for reaction 1 with M = Pd, for example, are shown in Figure 1. At such a four-centered TS, bond exchange is facilitated by the orbital interaction shown in 7, in which an occupied σ_{MH} and a vacant σ_{MH}^* orbital interact with π^* and π orbital of olefin, respectively. Formally, $d_{x^2-y^2}$ is vacant in the d^8

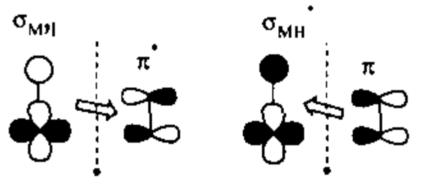

7

square-planar complex, 1, and thus the σ_{MH}^* orbital is vacant. Otherwise, the interaction between π and σ_{MH}^* would lead to unfavorable four-electron exchange repulsion. The same conclusion was obtained in the previous theoretical calculations as well as from frontier orbital arguments.[15-19]

In the structure of 2 with M = Pd (Figure 1), structural features for the agostic interaction,[20] an intramolecular CH···M interaction, are found: a long C–H bond of 1.13 Å, a short Pd···H distance of 2.13 Å, and the small Pd–C–C angle of 88°. While a three-center

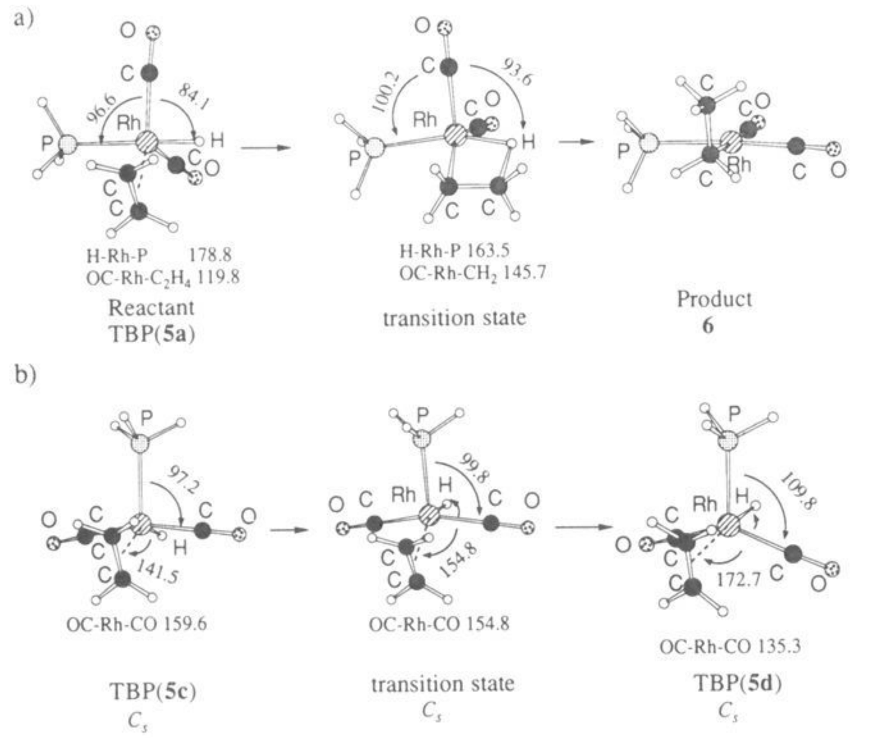

Figure 2. Structures (in angstroms and degrees), optimized at the RHF–ECP level, of reactant, product, and transition state for (a) ethylene insertion and (b) Berry pseudorotation of $Rh(H)(CO)_2(PH_3)(C_2H_4)$ (**5**).[13]

two-electron bond has been proposed experimentally as the basis of the M···CH interaction,[22] Koga, Kitaura, Obara, and Morokuma have found that this interaction is caused by electron donation from the β-C–H bond to an empty d orbital of the central transition metal (**8a**). They have also discussed the effect of this interaction on β-hydrogen elimination, the reverse reaction of olefin insertion,[11a] finding that it incipiently activates the C–H bond to lower the activation energy for β-hydrogen elimination. It has been also pointed out that electron back-donation from the σ_{MC} to the $\sigma_{CH}{}^*$ orbital (**8b**) is needed to complete β-hydrogen elimination at the later stage of reaction. Koga, Obara, and Morokuma have shown that the same electron donation causes the agostic interaction in $Ti(H)(C_2H_5)(Cl)_2(PH_3)_2$.[21a,b] Koga and Morokuma have also studied the C–Si···Ti intramolecular interaction, finding that a coordinatively unsaturated transition metal interacts not only with a CH bond but with other electron-donating σ bonds such as a C–Si bond.[21c]

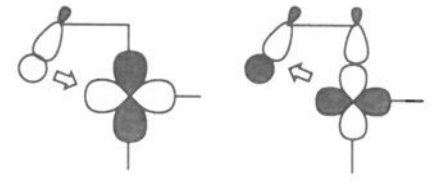

8a 8b

Reaction 2 is the rate-determining step of olefin hydrogenation by the Wilkinson catalyst.[23] The reactant of reaction 2, **3**, has a vacant d orbital, appropriate for the above interaction. However, the activation energy for reaction 2 is much larger, because of the high endothermicity. The details will be discussed in section III.

Reaction 3 is more complicated, since the Berry pseudorotation (BPR)[24] may isomerize the reactant with a low activation barrier. Koga, Jin, and Morokuma (KJM) have shown that when two TBP isomers are energetically close to each other, the activation energy for BPR connecting them is quite small.[13] It has also been found that the isomers having apical hydride and equatorial ethylene are more stable than the others. While apical hydride can use the vacant d_{z^2} orbital shown in **9** to form a strong Rh–H bond, equatorial ethylene is favorable because of strong π back-donation.[13,25]

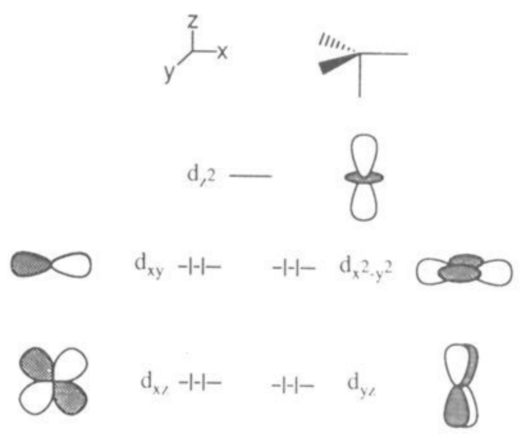

9

KJM have shown that ethylene insertion proceeds through the square-pyramidal TS as shown in Scheme I and Figure 2.[13] The skeleton of this square-pyramidal TS is similar to that of the TS for BPR also shown in Figure 2. This suggests that ethylene insertion couples with BPR. At this square-pyramidal TS the d orbital **10** is vacant and thus it can play the same role as $d_{x^2-y^2}$ in the d^8 square-planar complex.

SCHEME I. Potential Energy Profile for Ethylene Insertion of $Rh(H)(CO)_2(PH_3)(C_2H_4)$ (5) (numbers are RHF (MP2) energies relative to 5a)

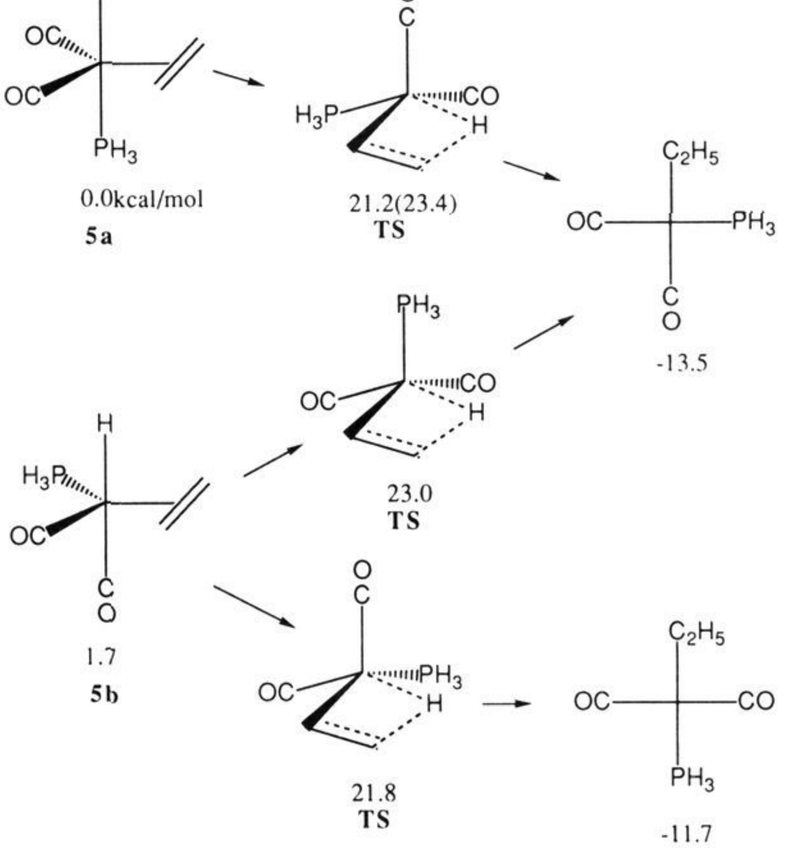

10

Antolovic and Davidson (AD) have also studied ethylene insertion of a d^8 five coordinate complex (reaction 4).[26] While they have optimized the structures

$$HCo(CO)_3(C_2H_4) \rightarrow C_2H_5Co(CO)_3 \tag{4}$$

of the reactant and the product at the RHF level, they follow the reaction path using the linear synchronous transient (LST) method. In the LST path, structures are linearly interpolated between the reactant and the

TABLE II. Energy of Reaction (ΔE) and Activation Energy ($\Delta E^{\ddagger}$) (in kcal/mol) of Ethylene Insertion into the Ti–CH$_3$ Bond of $X_2TiCH_3^+$[a]

X	symmetry	method	$\Delta E^{\ddagger}$	ΔE	ref
Cl	C_s	RHF	11		29
Cl[b]	C_s	RHF	12	−2	30
Cl	C_1	RHF	14	−3	31
		RMP2	6	*c*	31
		DPUMP2[d]	4	−11	31
Cp[b]	C_s	RHF	22		30
		RMP2	10	−12	30

[a] Optimized at the RHF level. [b] Optimized with the PRDDO approximation. [c] Second-order perturbation method could not be applied. [d] Doubly projected unrestricted MP2.

product. The LST path does not go through a square-pyramidal structure, which is the TS in reaction 3. Probably, this is the reason why their activation energies (38–51 kcal/mol at the RHF level and 39–55 kcal/mol at the SDCI level) calculated from the highest energies on the LST paths are much higher than those found for reaction 3. Reaction 4 has been studied also by the HFS method.[27]

Olefin insertion into an M–R bond is also very important, since it is a key reaction in the chain-growth step of olefin polymerization such as Ziegler–Natta polymerization.[1] The early ab initio MO study of C_2H_4 + $CH_3TiCl_4AlCl_2$ by Novaro, Blaisten-Barojas, Clementi, Giunchi, and Ruiz-Vizcaya has shown that the activation energy of insertion relative to the ethylene complex is low.[28] They have not used the energy gradient nor taken electron correlation into account. Therefore, their results should be considered to be rather qualitative. On the other hand, model reaction 5 has been studied by several groups with the energy gradient method.[29–31] The results are summarized in Table II.

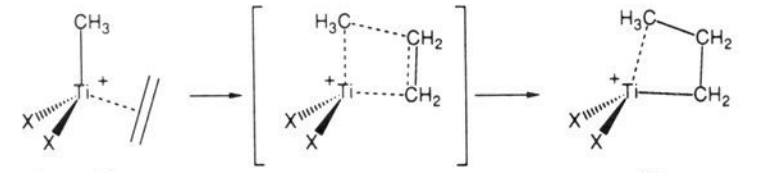

(5)

X=Cl 11
Cp 13

TS

12
14

Fujimoto, Yamasaki, Mizutani, and Koga have studied reaction 5 with X = Cl.[29] They have optimized the TS structure at the RHF level under the C_s symmetry constraint to show that the TS structure is four-centered as expected and that the activation energy is low (10.5 kcal/mol). They have also discussed the orbital interaction between $Cl_2TiCH_3^+$ and C_2H_4 using paired interacting orbitals to point out the importance of vacant d orbital participation just as in ethylene insertion into an M–H bond shown above.

Jolly and Marynick have studied reaction 5 with X = Cl and Cp (cyclopentadienyl).[30] They have determined the structures at an approximate ab initio level with the partial retention of diatomic differential overlap (PRDDO) approximation under the C_s symmetry constraint and have followed the reaction coordinate using linear synchronous transit/partial optimization approach. The activation energy for X = Cl at the ab initio RHF level was calculated to be 11.9 kcal/mol. For X = Cp the activation energy calculated was 22.1 kcal/mol at the RHF level and 9.8 kcal/mol at the MP2 level.

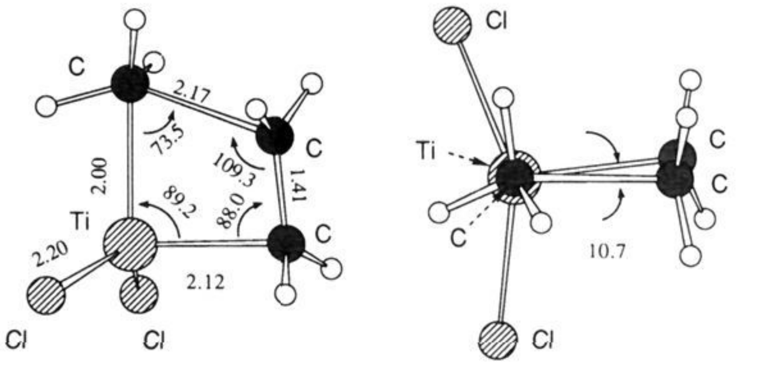

Figure 3. Structures (in angstroms and degrees), optimized at the RHF level, of transition state for ethylene insertion into the Ti–CH$_3$ bond of $Cl_2TiCH_3^+$ (eq 5).[31]

The above two studies have shown that the polymer propagation step is quite easy in these model catalysts. However, at the C_s transition state all the CH bonds of the propyl group are eclipsed and thus this TS may be unfavorable.

Kawamura-Kuribayashi, Koga, and Morokuma (KKM) have studied reaction 5 with X = Cl without any space-symmetry restriction, finding that the four-centered TS is slightly nonplanar, presumably to avoid eclipsing of CH bonds as shown in Figure 3.[31] The UMP2 calculation with triplet and quintet projection (DPUMP2) gave the activation energy of 4.3 kcal/mol; the reaction from the ethylene complex can take place easily. They included the electron correlation effect at the DPUMP2 level because the RHF wave function was unstable with respect to the UHF wave function, due to the strong covalent character of the relevant Ti–C bonds. In fact, the RMP2 energy was too low, showing that the RMP2 result is far from convergence of the perturbation series.

KKM have also studied propylene insertion by replacing one of the hydrogen atoms in ethylene by a methyl group. As shown in Scheme II, they have found that the primary, i.e. head-to-tail insertion is easier than

SCHEME II.[a]

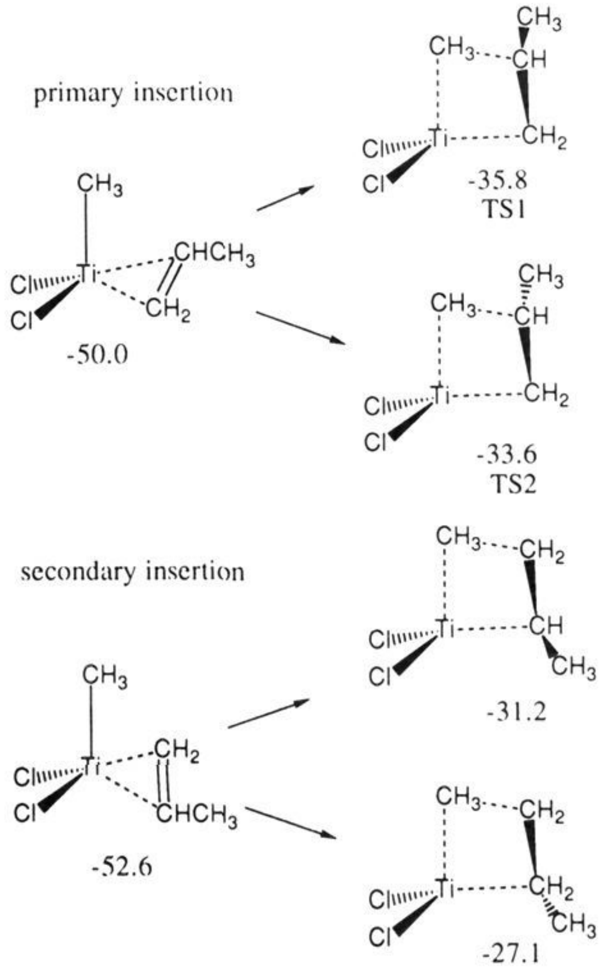

[a] Energies in kcal/mol relative to the reactants.

the secondary insertion, in agreement with the experimental situation and the Markovnikov rule of organic chemistry. In addition, they have found that nonplanarity of the transition state would give rise to stereoselectivity; TS1, with a methyl group located in the less-crowded region, is more stable than TS2.

B. Carbonyl Insertion

Carbonyl insertion into an M–R bond, which is also called migratory insertion, has been implicated in various catalytic cycles as one of the key steps.[1] There are two possible reaction pathways: (i) migration of the group R to the carbonyl or (ii) literal CO insertion into the M–R bond. As shown later, theoretical calculations have clearly demonstrated that the group R migrates to CO in late or middle transition metal complexes.

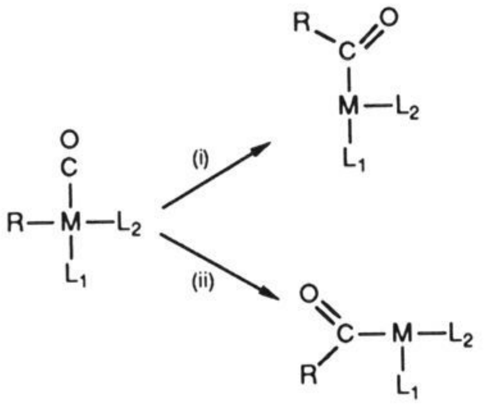

When the migrating groups are alkyl, aryl, and alkenyl, insertion has been observed to take place in many transition-metal complexes.[1] On the other hand, the hydride migratory insertion (eq 6) has been known only for a few cases in transition-metal complexes,[32,33] although it is believed to take place in homogeneous catalytic reactions of carbon monoxide reductive hydrogenation.[32] In the actinide complex hydride migratory insertion can take place easily as in the example of reaction 7.[34] The exothermicity of 2 kcal/mol of this reaction has been ascribed to the oxophilicity of Th which favors the η^2-formyl complex. The difficulty of hydride migratory insertion has been considered to be due to the stronger M–H bond, which makes hydride migratory insertion endothermic.[35] Although the hydride migratory insertion may be difficult to study experimentally, it can be studied theoretically and compared with alkyl migratory insertion, as shown later.

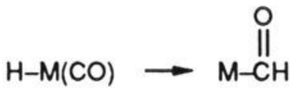

$$\text{H–M(CO)} \longrightarrow \text{M–}\overset{\overset{\text{O}}{\|}}{\text{C}}\text{H} \qquad (6)$$

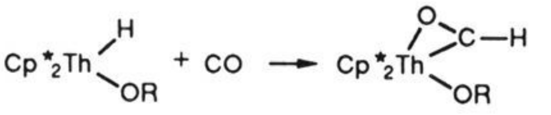

$$\text{Cp}^*_2\text{Th}(\text{H})(\text{OR}) + \text{CO} \longrightarrow \text{Cp}^*_2\text{Th}(\eta^2\text{-OCH})(\text{OR}) \qquad (7)$$

In an early ab initio MO study, the reaction of square-planar complexes of group 10 transition metals have been investigated. Sakaki, Kitaura, Morokuma, and Ohkubo have studied reaction 8 at the RHF–ECP level.[36] While they have optimized the structures of

$$\text{Pt(CH}_3\text{)(F)(CO)(PH}_3\text{)} \ (\textbf{15}) \rightarrow \text{Pt(COCH}_3\text{)(F)(PH}_3\text{)} \ (\textbf{16}) \quad (8)$$

the reactant and the product, they have changed the geometry of the reaction system stepwise to simulate three reaction paths, one for methyl migration, one for carbonyl migration, and one for concerted migration of CO and methyl with simultaneous opening of the FPtP angle as shown in Scheme III. From the energy change along the assumed paths, they concluded that methyl migration was the easiest and carbonyl migration was the most difficult.

SCHEME III.[a]

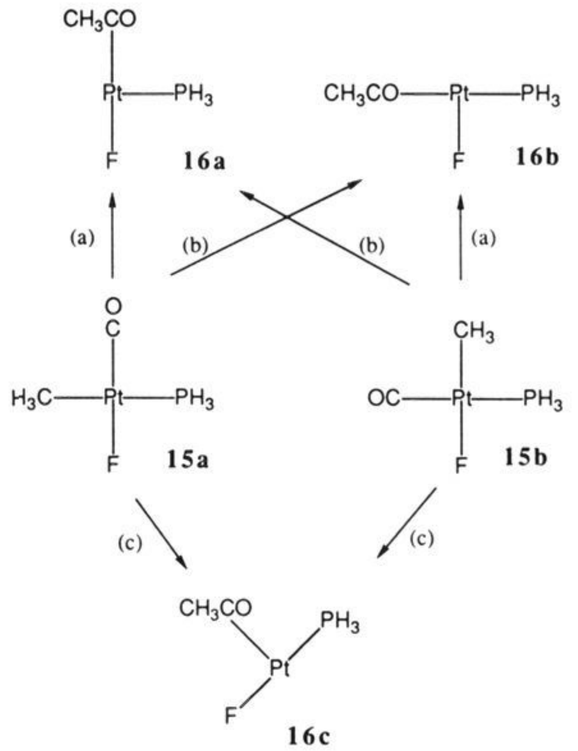

[a] (a) CH_3 migration. (b) CO migration. (c) Concerted migration of CH_3 and CO.

Koga and Morokuma have studied the carbonyl insertion reaction 9 of d^8 square-planar complexes.[11b,37]

$$\text{M(CH}_3\text{)(H)(CO)(PH}_3\text{)} \longrightarrow \text{M(COCH}_3\text{)(H)(PH}_3\text{)} \qquad (9)$$

M = Pd	**17**	**18**
M = Pt	**20**	**20**

Their structure determination with the energy gradient method at the RHF–ECP level has shown that the TS is three-centered and that the methyl group migrates toward the CO group as shown in Figure 4. The orbital interaction stabilizing the three-centered TS is shown in **21a**,[37,38] in which the sp^3 hybrid orbital of the migrating CH_3 group interacts with π^* of CO and the vacand d of the transition metal fragment. This interaction also suggests that an unstable d orbital and a stable π^* orbital would favor the migration.[39,40] On the other hand, the repulsion between the CO lone pair and the occupied d orbital would hinder carbonyl insertion into the M–R bond as shown in **21b**.[37,38]

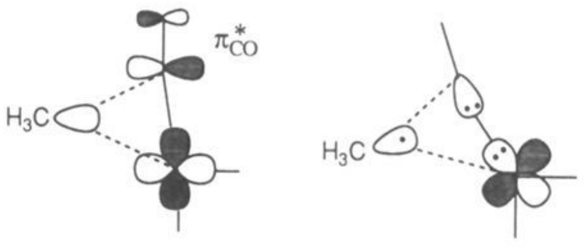

21a **21b**

Koga and Morokuma have also compared the reactivity in reaction 9 between Pd and Pt on the basis of the metal–ligand bond energy.[37] The energetics calculated is shown in Table III. In the carbonyl insertion reaction, an M–R and an M–CO bond are broken, an M–COR and an R–CO bond are formed, and the CO triple bond changes into a double bond. Among these bonds, the bond energy of the first three metal–ligand bonds would change, when the central transition

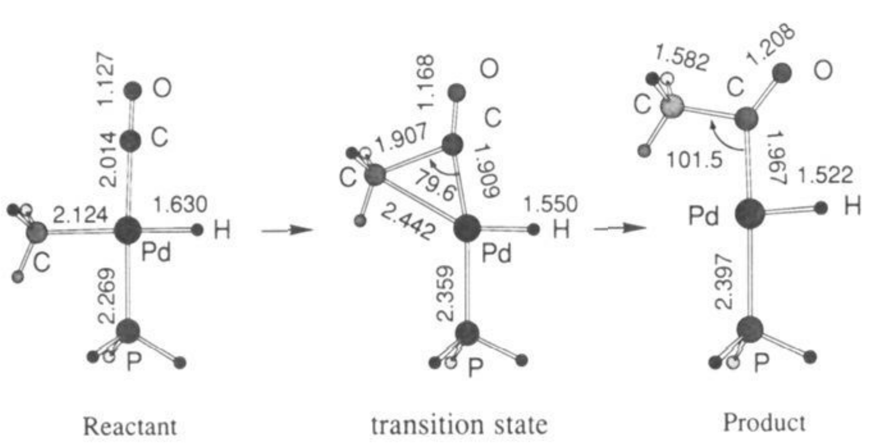

Figure 4. Structures (in angstroms and degrees), optimized at the RHF–ECP level, of reactant, 17, product, 18, and transition state for carbonyl insertion (eq 9).[37]

TABLE III. Energy of Reaction (ΔE) and Activation Energy ($\Delta E^{\ddagger}$) (in kcal/mol) of Carbonyl Insertion for (i) $Pd(CH_3)(H)(CO)(PH_3) \rightarrow Pd(COCH_3)(H)(PH_3)$, (ii) $Pt(CH_3)(H)(CO)(PH_3) \rightarrow Pt(COCH_3)(H)(PH_3)$, and (iii) $Pd(H)_2(CO)(PH_3) \rightarrow Pd(CHO)(H)(PH_3)$[a]

	method	$\Delta E^{\ddagger}$	ΔE (η^1)	ref
i	RHF/I	25.7	19.1	37
	RHF/II	18.8	5.0	37
	MP2/II	13.5	8.8	37
	RHF/III	22.0	10.6	49
	MP2/III	10.2	4.3	49
ii	RHF/I	31.3	23.0	37
	RHF/II	24.4	7.9	37
	MP2/II	21.8	17.6	37
iii	RHF/I	26.9	25.4	49
	RHF/III	19.2	17.7	49
	MP2/III	8.2	9.4	49

[a] The basis sets used consists of (I) [2s2p2d]/(3s3p4d) for Pd, [2s2p2d]/(3s3p3d) for Pt, effective core potential for Pt and Pd, 3-21G for CH_3, CO, and hydride, and STO-2G for PH_3, (II) [2s2p2d]/(3s3p4d) for Pd, [2s2p2d]/(3s3p3d) for Pt, effective core potential for Pd and Pt, [3s2p]/(9s5p) for C and O, [2s]/(4s) for all the hydrogens, and [6s4p]/(11s6p) for P, and (III) [2s2p3d]/(3s3p4d) for Pd, [2s3p2d]/(3s3p3d) for Pt, effective core potential for Pd and Pt, [3s2p1d]/(9s5p1d) for C and O, [6s4p]/(11s6p) for P, [3s1p]/(5s1p) for the hydride, and [2s]/(4s) for the other hydrogens. All the structures were optimized at the RHF/I level.

TABLE IV. Energy of Reaction (ΔE) and Activation Energy ($\Delta E^{\ddagger}$) (in kcal/mol) of Carbonyl Insertion of $RMn(CO)_5$

method	$\Delta E^{\ddagger}$	ΔE (η^1)	ΔE (η^2)	ref
		R = CH_3		
HFS	21	18	−1	43
PRDDO	18	1	−20	40
RHF[b]		3		40
RHF[c]	17	10	−1	40
		R = H		
RHF[a]	14	11		38
SDCI[a]	39	38		38
HFS	40	38	22	43
PRDDO	20	14	−5	40
RHF[b]		18		40
RHF[c]		26	15	40

[a] The basis functions used are [5s3p3d]/(13s8p6d) for Mn, [3s2p]/(9s5p) for C and O, and [3s]/(6s). [b] The basis set used is double-ζ for 3s, 3p, 4s, and 4p and triple-ζ for 3d for Mn and the 4-31G for C, O, and H. [c] The d polarization functions on C and O are added to the last basis set.

metal is replaced. Their analysis has shown that all the Pt–C bonds are stronger than the corresponding Pd–C bonds due to the relativistic effect. Therefore, the Pt carbonyl insertion is less favorable, in which two strong Pt–C bonds are broken and only one strong Pt–C bond is formed.

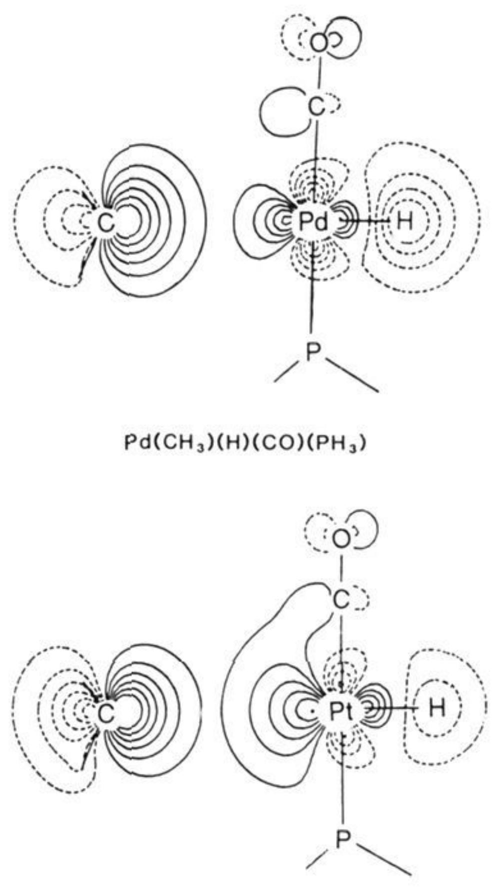

$Pd(CH_3)(H)(CO)(PH_3)$

$Pt(CH_3)(H)(CO)(PH_3)$

Figure 5. Interactive hybrid molecular orbitals of CH_3 and $M(H)(CO)(PH_3)$ for (left) M = Pd and (right) M = Pt.[37] To avoid overcrowding of contours, the separation between the two fragments in the figure is taken to be larger than the real interfragment distance.

As discussed in the Introduction, the relativistic effect stabilizes an s orbital. Since the heavier Pt atom has the larger relativistic effect, the Pt s orbital is expected to participate in bonding more effectively than the Pd s orbital, thus making the Pt–C bond stronger. In Figure 5 are shown the interactive hybrid MOs[29,41] the pairs of orbitals responsible for the M–CH_3 bonds in the reactants. One can see, as expected, the larger s orbital participation in the Pt–CH_3 bond.

Carbonyl insertion into the Mn–R bond has been well studied experimentally.[42] Carbonyl insertion of a Mn complex (eq 10) has been studied by several groups theoretically. The results of methyl and hydride migration are summarized in Table IV, which also includes the HFS results.[43]

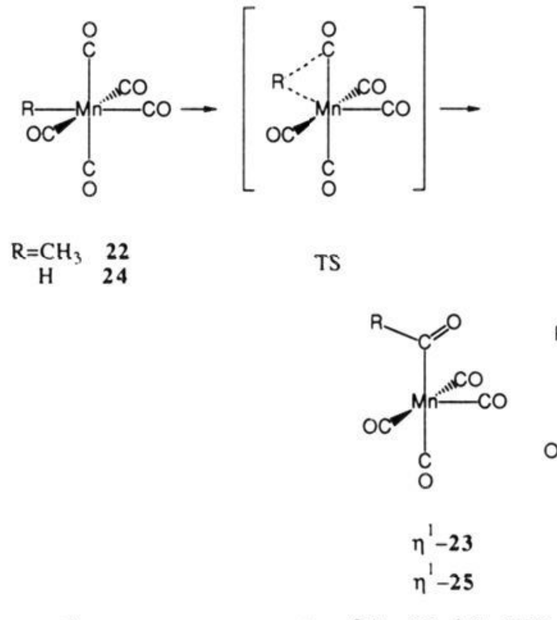

(10)

Axe and Marynick (AM) have studied the methyl migration.[40b] They have determined the TS structure at the PRDDO level and calculated the energetics at the full ab initio RHF level, showing that methyl migration takes place and that the orbital interaction

TABLE V. Energy of Reaction (in kcal/mol) of Carbonyl Insertion at Several Levels of Calculation

reactant	SCF	CASSCF4	CASSCF10	MP2	SDCI	ref
HMn(CO)	2.3^{a}	15.1	35.5	35.5	23.3	46
	11.5^{b}				27.4	48
	13.9^{c}					48
	7.4–15.2^{d}					47
	19.5–25.4^{e}					47
$CH_3Mn(CO)$	−1.8^{a}			36.4		46
$HPd(CO)^+$	−10.2^{a}	−21.4	−33.6	−15.8		46

[a] The basis functions used are [5s3p3d]/(13s8p6d) for Mn, [6s4p5d]/(15s9p8d) for Pd, [3s2p]/(9s5p) for C and O, and [3s]/(6s) (basis set I). [b] One set of p and d polarization functions on H, C, and D are added to the basis set I. [c] Two sets of p and d polarization functions on H, C, and O are added to the basis set I. [d] The basis sets used do not include polarization functions. [e] The basis sets used include polarization functions.

shown in **21a** is important. Also, they have found that the η^2-acyl complex is more stable than the η^1-acyl complex. A similar conclusion on the preference of η^2-acyl complex has been obtained by the HFS method.[43]

In the methyl migrations 8, 9, and 10 the activation barrier for the reverse decarbonylation reaction is substantial and thus the η^1-acyl complex is stable with respect to decarbonylation. On the other hand, the situation in hydride migration is different from this trend.

Nakamura and Dedieu (ND) have studied reaction 10 with R = H.[38] They have determined at the RHF level the reaction path by partial geometry optimization without using the energy gradient technique, finding that the mechanism is hydride migration. Along this reaction path, they have carried out more reliable single–double excitation configuration interaction (SDCI)[44] calculations to include the electron correlation effect. Then, they have found that the barrier is 39 kcal/mol and that the endothermicity is 38 kcal/mol, suggesting that hydride migration is quite difficult and even if the hydride migrates, the reverse reaction would take place with a very small barrier. The reason why hydride migration rather than CO insertion takes place is explained by the repulsive orbital interaction shown in **21b**.[38b]

AM have compared methyl and hydride migration of the Mn complex using the PRDDO and the ab initio RHF method.[40a] Their results have shown that the more endothermic hydride migration may be ascribed to the stronger Mn–H bond rather than to the Mn–CH_3 bond. The former is calculated to be stronger by about 20 kcal/mol.

The calculations by ND have shown that electron correlation increases the activation barrier by 25 kcal/mol and the endothermicity by 27 kcal/mol. Dedieu, Sakaki, Strich, and Siegbahn (DSSS) have studied this large difference in energetics between RHF and CI potential energy surface by investigating the carbonyl insertion of RMn(CO) (R = H, CH_3) and $HPd(CO)^+$ with the RHF, complete active space (CAS) SCF,[45] and MP2 method as shown in Table V.[46] As a result, DSSS have ascribed the large correlation effect to unbalanced description of π back-donation between the reactant Mn–CO bond and the product Mn–CHO bond at the RHF level. Although both in-plane and out-of-plane π back-donation take place in the reactant, only out-of-plane π back-donation takes place in the product, since the in-plane CO π^* orbital changes to the C–H σ bond orbital during the reaction. The RHF level of calculation, unable to describe the π back-donation properly, artificially destabilizes the reactant in the Mn complex. DSSS have found that π back-donation is not as important in the Pd(II) complex as in the Mn(I) complex, because the d orbital of Pd(II) is more stable than that of Mn(I) due to the higher oxidation number. This results in a smaller correlation effect in the Pd reaction. DSSS have concluded that the correlation effect may vary according to the nature and oxidation state of the transition-metal atom. The importance of d polarization function for a quantitative calculation of the Mn complex has been pointed out.[47,48]

Koga and Morokuma have adopted the hydride migration reaction 11 to compare the reactivity directly with methyl migration 9, where the ligand trans to the migrating group is the same in both reactions.[49] The

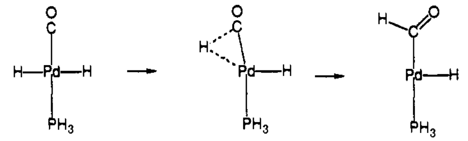

26 TS **27** (11)

energetics is shown in Table III. Hydride migration 11 is slightly more endothermic than methyl migration 9 at the MP2 level. This larger endothermicity of reaction 11 has been ascribed to the fact that the Pd–H bond is stronger than the Pd–CH_3 bond by 5 kcal/mol, although this difference is much smaller than that between the Mn–CH_3 and the Mn–H bond discussed above. Compared with hydride migration of the Mn complex (eq 10), reaction 11 is much less endothermic, since the back-donation in the Pd(II) complex is weaker than in the Mn(I) complex as discussed by DSSS. At the MP2 level, the barrier for the decarbonylation becomes negligible. In fact the geometry optimization with the MP2 energy gradient has shown that the potential energy surface is downhill for decarbonylation, indicating that the η^1-formyl complex is kinetically unstable. The three-centered interaction at the three-centered "TS" is stabilized by the orbital interaction similar to **21a**, in which the spherical 1s orbital could strongly interact simultaneously with the CO π^* orbital and the spd hybrid orbital of the transition metal. This nondirectionality of the hydride 1s orbital would make the transition state disappear. The fact that the hydride migration is uphill is probably the reason why the formyl complex is not detected. However, the endothermicity of hydride migration is low enough for the formyl complex to be an important transient species in catalytic processes.

The effect of substituent on the migrating alkyl group has been studied by Koga and Morokuma (KM) in re-

TABLE VI. **Effects of Migrating Group on Energy (ΔE) and Activation Energy ($\Delta E^{\ddagger}$) (in kcal/mol) of Carbonyl Insertions (reactants are Pd(R) (CO) (H) (PH_3) and $RMn(CO)_5$)**

	$\Delta E^{\ddagger}$	ΔE (η^1)	ΔE (η^2)	ref
		$Pd(R)(CO)(H)(PH_3)$[a]		
CH_2CH_3	23	15		37
CH_3	26	19		37
H	27	25		49
CHF_2	41	31		37
		$RMn(CO)_5$[b]		
CH_2CH_3		−8		40
CH_3		3 (10)	(−1)	40
H		18 (26)	(15)	40
CF_3		26 (28)	(31)	40

[a] Calculated at the RHF level. [b] Calculated at the RHF level. Numbers in parentheses are with the PRDDO approximation.

action 9 with M = Pd[37] and Axe and Marynick (AM) in reaction 10 as shown in Table VI.[40a] KM have discussed the effect of substituents in terms of the M–R bond energies. KM have stated that electronegative substituents stabilize the alkyl ligand that has a negative charge, leading to the stronger M–R bond as shown in the larger endothermicity and the higher activation energy for difluoromethyl. AM's results are similar.

Reaction 12 has been considered to be an elementary step of the hydroformylation catalytic cycle (R = alkyl).[50] Antolovic and Davidson (AD) have determined

$$RCo(CO)_4 \rightarrow RCOCo(CO)_3 \qquad (12)$$

the structures of $HCo(CO)_4$ (**28**) and $HCOCo(CO)_3$ (**29**) by the RHF energy gradient method,[26] and have further followed the reaction path according to the LST procedure. They have found the activation energy larger than 50 kcal/mol, which is too high for a catalytic reaction. Probably, responsible for this from the computational aspect are the lack of electron correlation and the unoptimized TS structure. In addition, there are some problems in the RHF calculation for the Co-carbonyl complex;[51,52] the most stable RHF structure of **28** is TBP with equatorial H, while the experimental structures are TBP with apical H. Thus, their results are not conclusive. However, they have ascribed the difficulty of H migration to the strong M–H bond.

Rappé has studied hydride migratory insertion to CO in an early transition metal complex (eq 13).[53] This model reaction was chosen because of its simplicity.

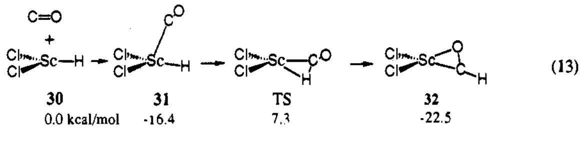

(13)

The structures of **30**–**32**, and the TS between **31** and **32** have been determined by the RHF energy gradient method. The energy calculations were carried out at the generalized valence bond (GVB)[54] and CI level of calculation. For the formyl complex, only the η^2 structure exists, which is more stable than the reactant complex, **31**. This is clearly in contrast to the Mn-formyl complex shown in reaction 10. Scandium is electron deficient and thus the bonding interaction between the lone pair of formyl oxygen and the empty d orbital of Sc has been found to favor the η^2 coordination. This is in agreement with the previous extended Hückel studies of an η^2-acyl complex[55] and the experimental observation of reaction 7.

There have appeared several studies in which a metal surface is modeled by a single transition metal. McKee, Dai, and Worley (MDW) have studied reaction 14[56] as a model carbonyl insertion on supported rhodium films.[57] Hydride migratory insertion from **33** has been

$$HRh(CO)\ (\mathbf{33}) \rightarrow Rh(CHO)\ (\mathbf{34}) \qquad (14)$$

calculated to be 29 kcal/mol endothermic and the conversion from **34** to **33** requires no activation energy at the MP3 level, the situation similar to hydride migration of $Pd(H)_2(CO)(PH_3)$ mentioned above and in agreement with the experimental fact that the formyl species has not been observed for supported Rh catalysts.[58] Pacchioni, Fantucci, Koutecky, and Ponec have studied reaction 15.[59] They have carried out SCF and

$$HM(CO)^n \rightarrow M(CHO)^n \quad M = Rh, Pd \quad n = 0, +1 \qquad (15)$$

CI energy calculations with the partial geometry optimization by using the ECP approximation, finding that hydride migration in a cationic system is easier than in a neutral system, in agreement with the experimental fact that the ion concentration is correlated with the catalytic activity.[60] It should be noted that their results are qualitatively different from MDW's for Rh[57] because of the use of a different, maybe poorer, ECP.

C. Other Insertions

The insertion of coordinated formaldehyde into an M–H bond has been assumed to take place in the homogeneous catalytic hydrogenation of carbon monoxide, which transforms synthesis gas into mono- and polyalcohols.[61] From the viewpoint of the orbital interaction, this insertion is similar to olefin insertion, since formaldehyde has a π and a π^* orbital as ethylene does. Consequently, it is expected that formaldehyde insertion could take place easily and would pass through a four-centered TS. Nakamura and Morokuma have determined the structures of the stationary points of reaction 16 at the RHF–ECP level with the energy gradient technique.[62] This hydride migration could give two intermediates, hydroxymethyl complex, **37**, and methoxy complex, **36**, from which ethylene glycol and methanol, respectively, are formed as the final products. They have found that the insertions pass through four-centered TSs as expected and that methoxy formation, **35** → **36**, is more exothermic than hydroxymethyl formation, **35** → **37**, by 23 kcal/mol at the RHF level. This difference has been attributed to the stronger M–O bond than the M–C bond. In addition

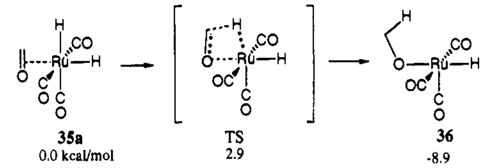

(16a)

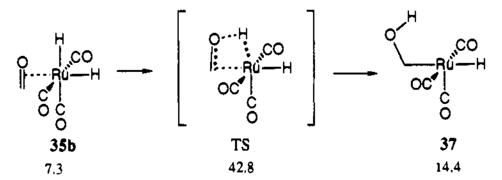

(16b)

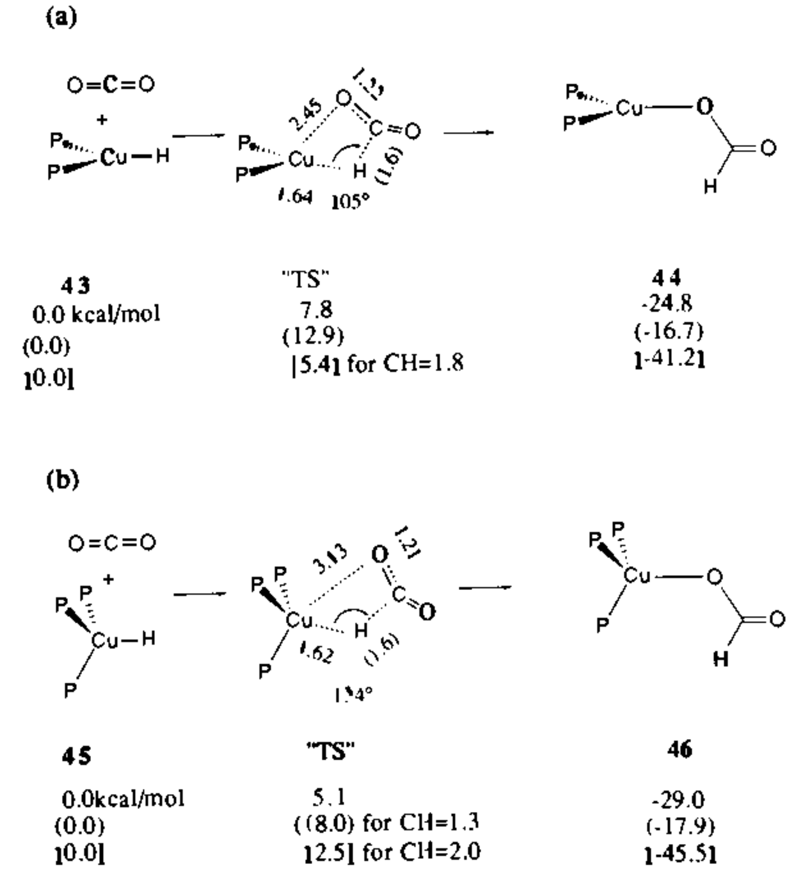

Figure 6. Potential energy profiles for CO_2 insertion to (a) $CuH(PH_3)_2$ (43) and (b) $CuH(PH_3)_3$ (45) calculated in kcal/mol at the RHF–ECP level, the MP2–ECP level (in round brackets) and at the all-electron RHF level (in square brackets), relative to the reactants.[65] The "transition state" structures (in angstroms and degrees) are those on the RHF-ECP potential energy curve and are optimized with the C–H distance fixed to be 1.6 Å. At the levels of calculation where the C–H distance at the corresponding TS is not 1.6 Å, the C–H distances are shown together with the activation energies.

to the energy of reaction, the lower activation energy of 2.9 kcal/mol favors methoxy formation. This low activation energy is ascribed to the large overlap between σ_{MH} orbital and the polarized π^* orbital shown in 38.

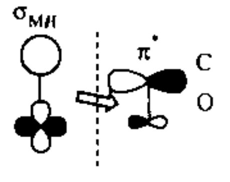

38

Introduction of CO_2 into organic substrates has drawn substantial attention, in connection with CO_2 fixation. CO_2 insertion into the M–X bond (X = H^-, CH_3^-, OR^-) has been experimentally studied.[63] CO_2 has π and π^* orbitals available for bond exchange and thus a four-centered TS is expected, if a vacant d orbital is available.

Bo and Dedieu (BD) have studied the interaction of CO_2 with $HCr(CO)_5^-$ and carried out a preliminary calculation of insertion reaction 17 at the all-electron RHF level.[64] The interaction of CO_2 with $HCr(CO)_5^-$ to give an adduct, 40, has been their main interest. The assumed η^2-HOCO structure, 41, which is considered to be similar to the true TS, is not high in energy. $HCr(CO)_4^-$ has a vacant d orbital, facilitating the bond exchange as discussed above. BD have concluded that insertion reaction from 40 coupled with CO dissociation may take place easily.

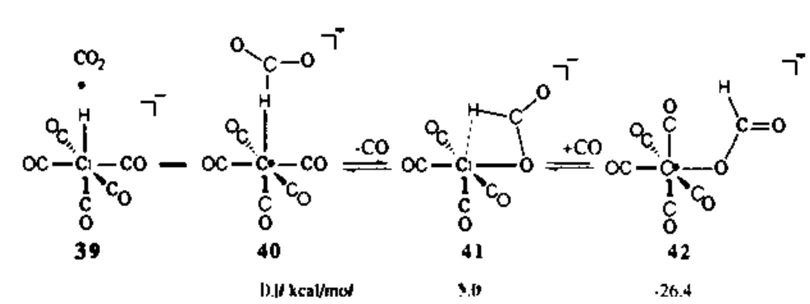

(17)

Sakaki and Ohkubo (SO) have studied CO_2 insertion into a Cu–H bond (eqs 18 and 19) at the RHF and RMP2 levels.[65] The TS's for both reactions were located at the Cu–H distance of 1.6 Å at the RHF–ECP level, whereas change of the basis set and inclusion of the electron correlation effect slightly shifted the position of the TS's.

$$CO_2 + HCu(PH_3)_2\ (\mathbf{43}) \rightarrow Cu(PH_3)_2(HCO_2)\ (\mathbf{44}) \qquad (\mathbf{18})$$

$$CO_2 + HCu(PH_3)_3\ (\mathbf{45}) \rightarrow Cu(PH_3)_3(HCO_2)\ (\mathbf{46}) \qquad (19)$$

Both reactions have been found to be exothermic with a low activation barrier and pass through a four-centered TS with a long Cu–O^1 distance as shown in Figure 6. SO have concluded that the origins of the activation barrier are the deformation of CO_2 and the exchange repulsion between $CuH(PH_3)_n$ and CO_2 and that the charge transfer from $CuH(PH_3)_n$ to CO_2 is important for stabilizing the reaction system. The additional phosphine in reaction 19 enhances the charge transfer from the CuH moiety to CO_2, resulting in a smaller energy being required in the early stage of reaction 19. Also, the polarization within $CuH(PH_3)_n$ and CO_2 moieties and the electrostatic interaction between O^1 and Cu cooperate in the formation of new bonds. Such interactions are shown in 47. From the viewpoint of orbital interaction, the O^1–Cu interaction is not favorable because of the out-of-phase combination. Note that Cu(I) is d^{10} and thus no vacant d orbital is available. Therefore, the Cu–O^1 distance is much longer, compared with the M–C distance in olefin insertion discussed in the previous section. In this regard, reactions of Cu(I) are different from those of transition-metal complexes having a vacant d orbital.

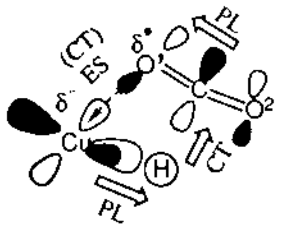

47

Hydride or alkyl migration to carbene ligand has been considered to be a key step of catalytic reactions.[66] In the CH_2 ligand, there is a vacant p_π orbital which can play the same role as the CO π^*. Carter and Goddard have studied reaction 20 at the HF, GVB, GVB–CI, and CASSCF levels of calculation.[67] At the highest level,

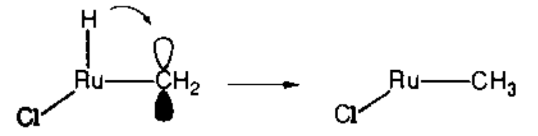

(20)

six-electron and six-orbital CASSCF, they have found an activation barrier of 12 kcal/mol with an exothermicity of 7 kcal/mol. The TS is three-centered, similar to that for hydride migration to CO. They have concluded that hydride migration to CH_2 is feasible for late transition metal complexes. The GVB wave function has shown that the Ru–H bond smoothly converts into the C–H bond with the aid of CH_2 p_π orbital.

D. Nucleophilic Additions to Coordinated Ligands

Nucleophilic additions to coordinated unsaturated compounds have been considered to be an important elementary reaction in catalytic reactions,[1] such as the Wacker process, aminopalladation of olefin, and oxymerculation. There have appeared several theoretical studies for nucleophilic addition by using ab initio as well as semiempirical method,[68–73] and mechanisms of activation of organic molecules coordinated to the transition metal have been discussed.

Dedieu and Nakamura (DN) have studied nucleophilic addition of hydride and methyl and hydroxy anion to carbonyl ligand of $Fe(CO)_5$ (eq 21).[70] In the case of hydride addition, DN have found that the hydride attacks the apical carbonyl and not the equatorial carbonyl and that the reaction is highly exothermic, with an energy of reaction of −69 kcal/mol. The selectivity of the apical carbonyl was ascribed to the interaction between the empty d_{z^2} orbital and the CHO lone pair orbital, which forms a Fe–CHO σ orbital as shown in **48**. This is the same as the hydride apical preference shown in section IIA. The empty d orbital is not available for equatorial carbonyl.

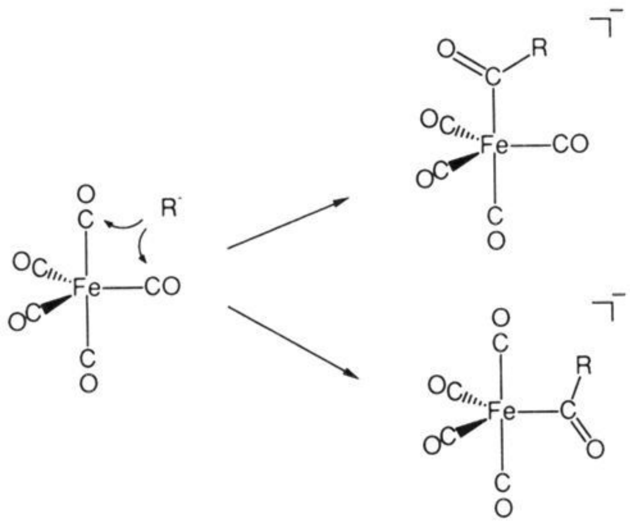

(21)

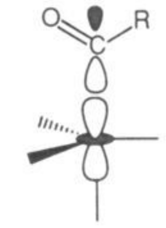

48

Nakatsuji, Ushio, Han, and Yonezawa (NUHY) have studied the electronic structure of Fischer-type and Schrock-type carbene complexes at the RHF level.[73] The complexes studied were $(CO)_5Cr{=}CH(OH)$ (**49**) and $(CO)_4Fe{=}CH(OH)$ (**50**) as models of the former and $H_2(CH_3)Nb{=}CH_2$ (**51**) as that of the latter. It is well known that nucleophiles attack the carbene carbon of the Fischer-type complex. NUHY have shown that the carbene carbons of **49** and **50** are negatively charged. They have thus concluded that this nucleophilic addition is not charge controlled but frontier orbital controlled. For the Schrock-type complex it is also known that nucleophiles attack the transition metal and that the carbene carbon receives electrophilic attack. This feature of reactivity had usually been explained by the charge control argument. However, their calculations have shown that the Nb atom as well as the carbene carbon have negative charge. Their analysis of molecular orbitals has again shown that the selectivity can be explained by frontier control argument. It should be noted, however, that DN have stated that the negative charge on the carbene carbon is an artifact of the minimal basis functions used by NUHY or of the Mulliken population analysis.[70b]

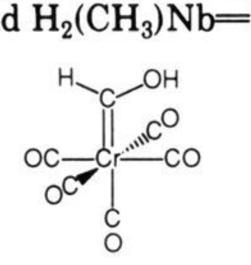

49

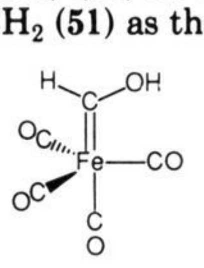

50

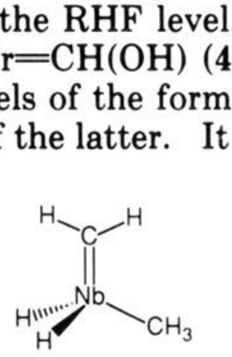

51

Sakaki, Maruta, and Ohkubo (SMO) have studied nucleophilic addition to the coordinated ethylene. The reactions studied were models of aminopalladation, addition of NH_3 to ethylene coordinated to $Pd^{II}F_m(NH_3)_{3-m}{}^n$ with $(m, n) = (1, +1), (2, 0)$, or $(3, -1)$ and $Pd^{II}F(PH_3)_2$, shown in **52**.[72a] SMO have found that nucleophilic addition to the cationic complex was easier than that to the neutral and anionic complex and have proposed that the cationic species is the active intermediate in the catalytic reaction. They have analyzed electron reorganization upon nucleophile attack. Nucleophilic addition to the cationic intermediate is easy because of the favorable electrostatic interaction, large charge transfer and small exchange repulsion. The reorganization of electron distribution is shown in **53**.

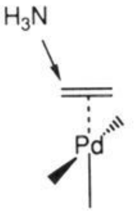

52

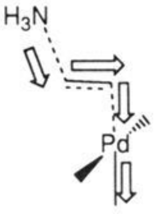

53

Fujimoto and Yamasaki have compared nucleophilic addition to ethylene coordinated to $PdCl_3^-$ and $PdCl_2(H_2O)$ using hydride and hydroxide anion as a model of nucleophile.[71] They also have shown that in the neutral system the lower lying vacant d orbital is more effectively used for charge transfer and polarization and for reduction of exchange repulsion, similar to the results by SMO.

SMO have also compared nucleophilic addition of H_2O to free ethylene, and ethylene coordinated to Li^+ and HgH^+ to show that only the reaction catalyzed by the cationic Hg complex is easy.[72b] They have concluded that the low-energy acceptor orbital of Hg accelerates nucleophilic addition.

E. Oxidative Addition and Reductive Elimination

Oxidative addition to and reductive elimination from transition-metal complexes are important elementary processes.[1] The former introduces an organic molecule into a catalytic cycle, and the latter gives an organic

TABLE VII. Energy of Reaction (ΔE) and Activation Energy ($\Delta E^{\ddagger}$) (in kcal/mol) of Oxidative Addition, A-B + [M] → A-[M]-B (numbers in parentheses were estimated values)

[M]	$\Delta E^{\ddagger}$	ΔE	ref
	A-B = H-H		
Ni(^{1}D)	3	−8	79[a]
Pd(^{1}S)	5	4	81[b]
	downhill	−4[f]	81[b]
	downhill	−6[f]	80[a]
	downhill	−15[f]	94a[c]
$Pd(PH_3)_2$	uphill	(22)	81c
$Pd(OH_2)_2$	–	−7	80[a]
$PdCl_2(PH_3)_2$	uphill	(38)	81c
Pt(^{1}S)	downhill	−34	81[b]
	downhill	−64	94c[c]
$Pt(PH_3)_2$	7	−27	75[d]
	8	−22	75[e]
	17	−5	76[d]
	2	−16	77[b]
$PtCl_2(PH_3)_2$	(6)	(−8)	81c
	A-B = CH_3-H		
Ni(^{1}S)	54	21	86[a]
Pd(^{1}S)	31	20	81[b]
$Pd(PH_3)_2$	uphill	(44)	81c
$PdCl_2(PH_3)_2$	uphill	(67)	81c
Pt(^{1}S)	13	−16	81[b]
$Pt(PH_3)_2$	30	−5	75[d]
	28	−5	75[e]
	(25)	7	81c[b]
$PtCl_2(PH_3)_2$	(32)	(22)	81c
	A-B = CH_3-CH_3		
Ni(^{1}S)	42	5	86[a]
Pd(^{1}S)	39	16	81[b]
$Pd(PH_3)_2$	(52)	43	81c
$PdCl_2(PH_3)_2$	uphill	(70)	81c
Pt(^{1}S)	35	−18	81[b]
$Pt(PH_3)_2$	(48)	8	81c[b]
$PtCl_2(PH_3)_2$	(57)	25	81c[b]

[a-d] Calculated by (*a*) the all-electron contracted CI method, (*b*) the GVB-CI method with the ECP approximation, (c) the symmetry adopted cluster expansion (SAC) method with the ECP approximation, (*d*) the SDCI method with the ECP approximation. [e] Zero-point energy correction was added to the SDCI result. [f] Energy for the weak H_2 complex formation.

compound as a product by coupling two ligands.

Oxidative addition of H_2 to a d^{10} transition-metal complex or a transition-metal atom is one of the simplest reactions, from the computational point of view, in organotransition-metal chemistry. Experimentally, oxidative addition of H_2 to d^{10} $Pt(PR_3)_2$ has been studied,[74] in which only a trans product has been observed. Seemingly contrary to this fact, the trans addition is symmetry forbidden, while the cis addition is symmetry allowed.

Several groups have studied model reactions of this simple oxidative addition (eq 22) using the ab initio MO method in order to clarify the electronic feature and the potential energy surface.[75-77,79-81] The results are

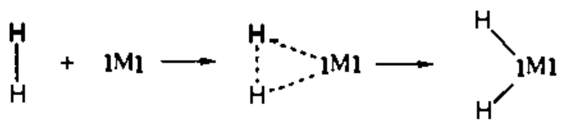

(22)

summarized in Table VII.

Kitaura, Obara, and Morokuma (KOM) have determined the TS structure of reaction 23 with the RHF-ECP energy gradient method and furthermore carried out the vibrational analysis, to show that the three-centered TS is a true TS, having one imaginary frequency.[75] This was the first theoretical determination of the TS structure of organotransition-metal reactions.

Irrespective of the computational methods, H_2 addition to $Pt(PH_3)_2$ (reaction 23) is exothermic with low activation energy as shown in Table VII. Recent kinetic studies of reductive elimination of H_2 from $H_2Pt(PMe_3)_2$ have shown that the activation enthalpy is 20 kcal/mol in noncoordinating solvents.[78] This is in agreement with the calculated activation energies for reductive elimination ($\Delta E^{\ddagger} - \Delta E$). The results of KOM are slightly different from the others, since in this early study a poorer ECP was used, which is more attractive than the other ECPs.

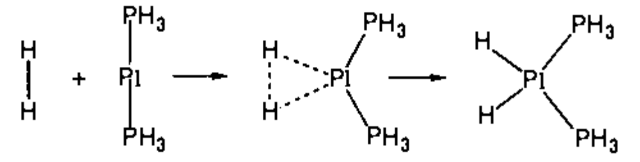

54 TS 55

(23)

The H-H distance at the three-centered transition state of reaction 23 ranges from 0.75 to 0.90 Å, not much longer than that in the free H_2; the TS is located in the early stage of reaction. At this TS, donation from σ_{HH} to sp hybrid of Pt and back-donation from the Pt-occupied d orbital to σ_{HH}^* facilitate bond exchange (56).

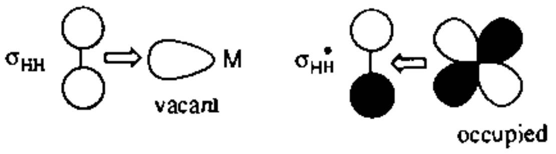

56

Oxidative addition of H_2 to Ni atom to give NiH_2 and reductive elimination from NiH_2 (eq 24) have been studied in the early theoretical studies by Blomberg and Siegbahn (BS).[79] BS have investigated with the

$$H_2 + Ni \rightarrow NiH_2 \qquad (24)$$

CASSCF and the contracted CI method potential energy surfaces of NiH_2 in several electronic states, which are different in space symmetry as well as in spin symmetry. The most interesting state is $^1A_1$, since oxidative addition and reductive elimination only in this state is symmetry allowed and is considered to be similar to those of H_2NiL_2 as well as H_2PtL_2. BS have found that NiH_2 ($^1A_1$) has a bent equilibrium structure with the H-Ni-H angle of 50° and the Ni-H distance of 1.43 Å. As anticipated for symmetry-allowed reaction, the activation energy of 3 kcal/mol for oxidative addition is low. The reaction is exothermic by 8 kcal/mol with respect to Ni(^{1}D) + H_2. They have found an interesting character of the Ni-H bond; the Ni orbital responsible for the Ni-H bond is 4s-3d hybrid and the formation of this hybrid is facilitated by the contribution of the atomic d^9s^1 electronic state which corresponds to the singlet ground state of Ni (^{1}D). Note that though formally oxidation state of Ni in NiH_2 is two, the calculations showed that Ni is almost neutral and that it has nearly 10 electrons.

The importance of the d^9s^1 electronic state in dihydride complex is also shown by Brandemark, Blomberg, Pettersson, and Siegbahn (BBPS)[80] and Low and Goddard (LG).[77] For Pd the d^9s^1 state is an excited state, whereas the ground state is d^{10} (Table VIII). Thus, the formation of Pd-H bond has been expected to be more difficult. BBPS have studied H_2 oxidative addition to Pd and $Pd(H_2O)_2$ with the all-electron

TABLE VIII. Pd and Pt Atom State Splittings (in kcal/mol) (numbers in parentheses are experimental values[a])

	d^{10}	d^9s^1	d^8s^2
Pd	−19.6 (−21.9)	0.0 (0.0)	62.6 (56.0)
Pt	12.3 (11.0)	0.0 (0.0)	17.2 (14.7)

[a] Reference 77. Calculated by the GVB-RCI method.

CASSCF and the contracted CI method. For Pd + H_2 BBPS have found only a weak H_2 molecular complex, in which the H–H distance is essentially that in the free H_2. In this weak complex, the H_2 molecule binds to the Pd atom through weak donation and back-donation. On the other hand, coordination of electron-donating H_2O was anticipated to raise the energy of d^{10} state relative to d^9s^1 and thus sd hybridization would become easier. In fact, upon coordination of H_2O, their calculations have shown that the dihydride complex $(H)_2Pd(H_2O)_2$ with the bond between Pd sd hybrid and H 1s orbitals is stable and that the oxidative addition leading to this dihydride complex is 7 kcal/mol exothermic. Note, however, that LG have found the dihydride Pd complex as well as the weak H_2 complex by using the relativistic ECP.[81a] LG have concluded that the relativistic effect stabilizes d^9s^1 relative to d^{10}, to make the Pd–H bond formation easier than in the nonrelativistic all-electron calculation. However the dihydride complex is less stable than the weak H_2 complex in their calculation.

LG have found in their study of reaction 23 that the sd hybrid forms the Pt–H bond and have stressed that the Pt ground state of d^9s^1 (Table 8) favors H_2 oxidative addition.[81a] LG have also concluded that the Pd reaction is less favorable than the Pt reaction because of the unstable Pd d^9s^1 state.[81a] In later studies, LG have actually compared the energetics between the Pd and the Pt complex.[81b,c]

LG have considered that in oxidative addition from M(II) to M(IV) the electronic state of metal changes from d^9s^1 to d^8s^2. For Pt, the ground state is d^9s^1 and thus the process from Pt(II) to Pt(IV) is unfavorable as shown for $Pt(Cl)_2(PH_3)_2$ in Table VII, compared with that from Pt(0) to Pt(II). Blomberg, Siegbahn, and Bäckvall (BSB) have studied the ring opening of cyclopropane by Pd^0, $Pd^{II}Cl_2$, $Pd^{II}Cl_4^{2-}$, and $Pd^{II}Cl^+$.[82] BSB have shown that oxidative addition of cyclopropane to Pd^{II} requires a large activation energy and is very endothermic, reflecting the energy difference between atomic electronic states.

Since it has been experimentally found in $(\eta^2\text{-}H_2)W(CO)_3(PR_3)_2$ by Kubas et al.,[83] the molecular H_2 complex has been drawing substantial attention.[84] Hay has studied the structure and oxidative addition of the model complexes, $W(PH_3)_2(CO)_3(\eta^2\text{-}H_2)$ (**57**) and $W(PH_3)_5(\eta^2\text{-}H_2)$ (**58**).[85] Although this oxidative addition (eq 25) gives a seven-coordinate complex and thus is expected to be unfavorable, he has found that the oxidative addition of the latter complex is very exothermic. He has concluded that the electron-donating phosphines destabilize the d orbitals, thus enhancing back-donation which breaks the HH σ bond.

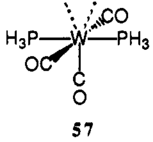

57

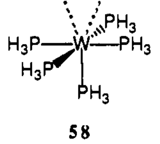

58

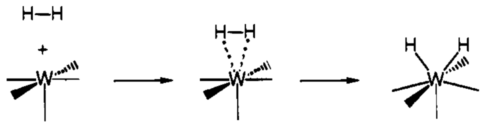

(25)

The rather small H–Ni–H angle of 50° found in NiH_2 (eq 24) by BS indicates bonding interaction between the hydrides. BS have concluded that the spherical 1s orbital of hydride stabilizes the three-centered interaction in NiH_2 and have considered that oxidative addition of CH_4 and C_2H_6 would require higher activation energy, since the directionality of the methyl sp^3 hybrid would not favor the three-centered interaction at the TS. Therefore, BS have compared the CH oxidative addition of CH_4 and CC oxidative addition of C_2H_6 to Ni with the CASSCF and the contracted CI method.[86] Their results have shown that CH_4 and C_2H_6 oxidative addition requires a larger activation energy than H_2 oxidative addition as shown in Table VII. LG have also found that the methyl group increases the activation energy.[81]

Consistent with unfavorable three-centered interaction among two alkyl groups and a transition metal, C–C bond formation by reductive elimination is in general difficult.[1] Koga and Morokuma have determined the stationary structures of reductive elimination 26a of the Rh dinuclear complex at the RHF–ECP level and compared them with those of the mononuclear complex (eq 26b).[87] They have found that the activation barrier is 42 kcal/mol at the MP2 level, 24 kcal/mol lower than reaction 26b of the mononuclear complex, and that reaction 26a is 10 kcal/mol less endothermic than reaction 26b. They have concluded that strain in the Rh–μ–CH_2 bond makes reaction 26a easier than reaction 26b.

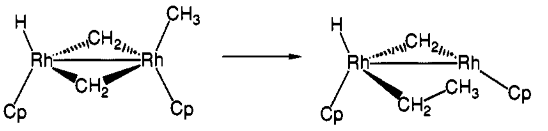

(26a)

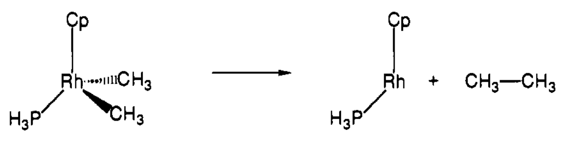

(26b)

In the above reactions (eqs 22–24), all the d orbitals of reactant are doubly occupied and thus electron donation takes place from organic molecule to the vacant sp orbital of the transition-metal complex. On the other hand, coordinatively unsaturated complexes having a vacant d orbital have recently been produced thermally or photochemically by ligand dissociation of reductive elimination. These have been found to activate a C–H bond easily.[88]

Koga and Morokuma have studied reaction 27 as a model of CH activation at the ab initio RHF and MP level.[89] **59** is a model complex of $RhCl(PR_3)_2$, which

$$CH_4 + RhCl(PH_3)_2\ (\mathbf{59}) \rightarrow HRhCl(PH_3)_2(CH_3)(\mathbf{60}) \qquad (27)$$

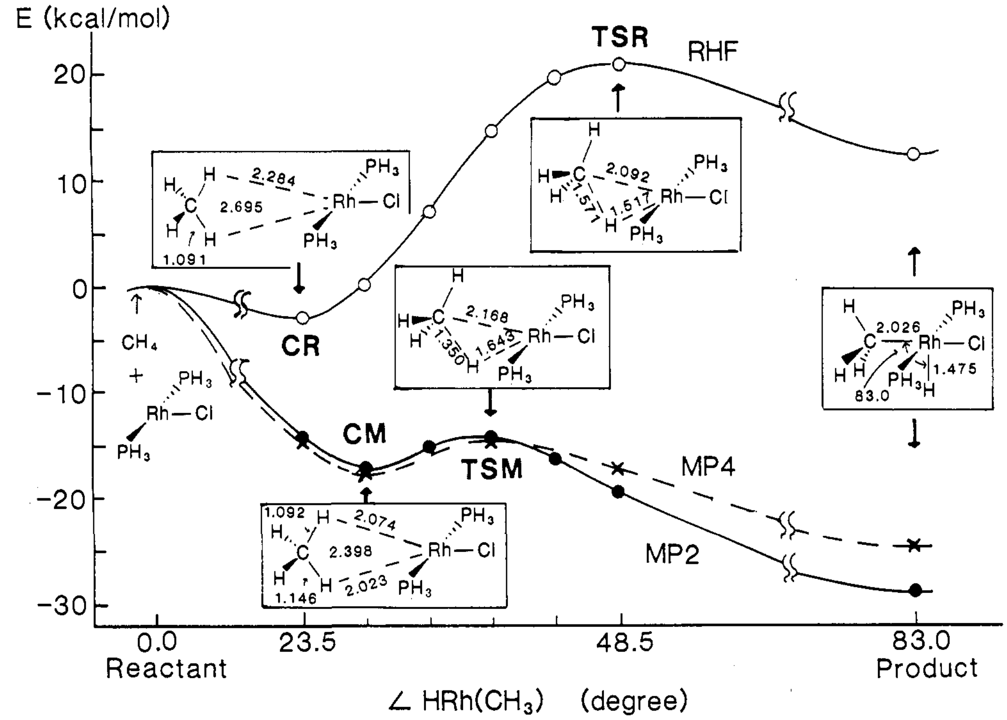

Figure 7. Potential energy curves for $CH_4 + RhCl(PH_3)_2 \rightarrow HRhCl(PH_3)_2(CH_3)$ with the optimized structures at important points. CR and TSR are the CH_4 complex and the TS optimized at the RHF level, whereas CM and TSM are those on the MP2 potential energy curve calculated by using several RHF optimized structures between CR and TSR.[89]

is a coordinatively unsaturated intermediate in the catalytic cycle of carbonylation of hydrocarbons.[90] They have found that the potential energy surface of reaction 27 is quite different from that for other oxidative additions; reaction 27 passes through the methane complex, in which two C–H bonds interact with Rh simultaneously, and the three-centered transition state is more stable than the reactants, while the activation barrier from the methane complex is very low as shown in Figure 7. In addition to back-donation from an occupied d orbital to $\sigma_{CH}{}^*$, donation from σ_{CH} to a vacant d orbital makes the interaction between CH_4 and $RhCl(PH_3)_2$ stronger than donation to an sp orbital. One can see the large correlation effect on the energetics in Figure 7; the MP2 and MP4 energy curves are completely different from the RHF energy curve. They have analyzed this correlation effect with the MP2 method based on localized MOs. As a result, they have found that the Rh–H and the Rh–C bond in the product are covalent and have a large d character and that the Rh–H and the Rh–C intrabond correlation as well as the correlation between these σ bonds and d electrons are consequently large.

Though some of the studies mentioned above discussed reactions of transition metal atoms, those reactions were regarded as models of reactions of transition-metal complexes. Recently, ion beam experiments have shown some interesting features of potential energy surfaces for reactions of atomic transition metal ions with organic compounds including H_2 and alkanes.[91] In addition, considerable attention has been paid to reactions of transition metal clusters, produced in rare gas matrices or in supersonic molecular beam, with a small molecule such as H_2. These have been considered as models of reactions on surfaces and clusters. Balasubramanian and his co-workers have studied potential energy curves for several electronic states of MH_2 (M = Sc, Pt, Pd, Y, Au, Ag, Nb, Tc^+, and Ru^+) with respect to bending angle at the CASSCF and the MRSDCI level.[92] Novaro et al. carried out the CI calculations of MH_2 (M = Cu, Pd, Ag, and Pt).[93] Nakatsuji et al. have studied potential energy surfaces of Pd_nH_2 and Pt_nH_2 (n = 1, 2, 3) to model catalysis on the metal surface.[94]

F. Metathesis

Olefin metathesis is one of the important reactions in organic synthesis, in which alkylidene units are exchanged between double bonds (eq 28). The active

$$R^1CH{=}CHR^2 + R^3CH{=}CHR^4 \leftrightarrow R^1CH{=}CHR^3 + R^2CH{=}CHR^4 \leftrightarrow R^1CH{=}CHR^4 + R^2CH{=}CHR^3 \tag{28}$$

intermediate in homogeneous system has been considered to be a carbene complex (eq 29).[1] Upton and

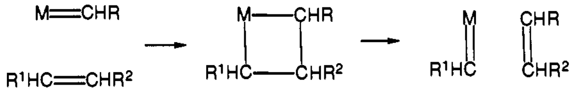

(29)

Rappé (UR) have studied isomerization of *Ti*,*Ti*-dichlorotitanacyclobutane (61) to ethylene–titanium methylidene complex (62) (eq 30).[95] *Ti*,*Ti*-Dicyclopentadienyltitanacyclobutane is a moderately active olefin metathesis catalyst.[96] Although they have found

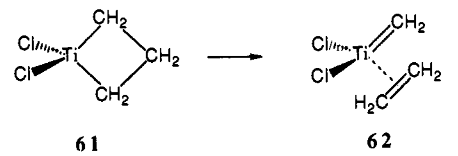

61 62 (30)

a TS connecting 61 and 62, the TS and 62 are essentially degenerate, the potential energy differences being only 2 kcal/mol and after the zero-point energy correction becoming zero. The absence of barrier for **62** → **61** is consistent with the experimental fact of no direct observation of methylene–olefin complex.[96] UR have demonstrated the role of the d orbital, which lowers the activation barrier drastically for [2s + 2s] addition reaction, well known to be symmetry forbidden in organic chemistry.

In metathesis such as reaction 29, olefin is a substrate and its π bond is broken to form a new C–C σ bond of metallacycle. Different from this olefin metathesis, σ metathesis, in which a σ bond interacts with a transition metal and is broken, has recently drawn attention.[97-100]

Steigerwald and Goddard have studied with the GVB method the hydrogen exchange reaction through a four-centered transition state as a model of [2s + 2s] addition such as olefin insertion (eq 31).[101] The calculated activation energy are 2, 22, and 17 kcal/mol for Ti$^+$, Ti, and Sc, respectively. While these low activation barriers show that this [2s + 2s] reaction takes place easily, an analysis of the GVB wave functions has shown that the larger the d character of the M–H bond, the lower the activation energy; the d character of the TiH bond in the Ti cationic system is 90%. This study has demonstrated that σ-bond exchange is a [2s + 2s] reaction and that H–D exchange can take place easily.

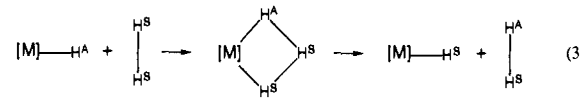

(31)

$[M]=Cl_2Ti^+$. Cl_2Ti. Cl_2Sc

Different from the H–H exchange reaction, in the reaction of metal hydride with alkene or alkyne, σ-metathesis competes with insertion reaction. Rappé has studied the reaction of scandium hydride with acetylene with the GVB and the CI method in order to compare these two reaction modes.[102] His calculations have shown that all the reactions pass through a four-centered transition state as shown in Figure 8 and that the participation of d orbitals leads to low activation energy. In particular, insertion reaction 32a requires an activation energy of only 6 kcal/mol and is exothermic by 9.1 kcal/mol. Although the activation energy of acetylide formation 32b through σ metathesis is also 6 kcal/mol, it is less exothermic and thus the reverse reaction would be allowed. On the other hand, H exchange 32c through σ metathesis requires a high activation energy and is thus unfavorable. Although these computational results are inconsistent with the experimental observation that only σ metathesis takes place[99] in the reaction of propyne with Cp^*_2ScR (R = H, CH_3) to produce acetylide, one can say that σ metathesis of early transition metal complexes is a facile reaction.

$$Cl_2ScH + HCCH \rightarrow Cl_2Sc{-}CH{=}CH_2 \quad (32a)$$

$$Cl_2ScH^A + H^BCCH \rightarrow Cl_2Sc{-}CCH + H^AH^B \quad (32b)$$

$$Cl_2ScH^A + H^BCCH \rightarrow Cl_2ScH^B + H^ACCH \quad (32c)$$

III. Catalytic Cycle

A reaction catalyzed by a transition-metal complex has been considered to be a sequence of elementary organometallic reactions as mentioned above. In early ab initio MO studies, catalytic cycles have been discussed based on the stability of intermediates. In some cases, structures of intermediates have not been determined theoretically, but some geometrical parameters were taken from the experimental structures or assumed. Although such studies are qualitative, some important information has been obtained as shown below.

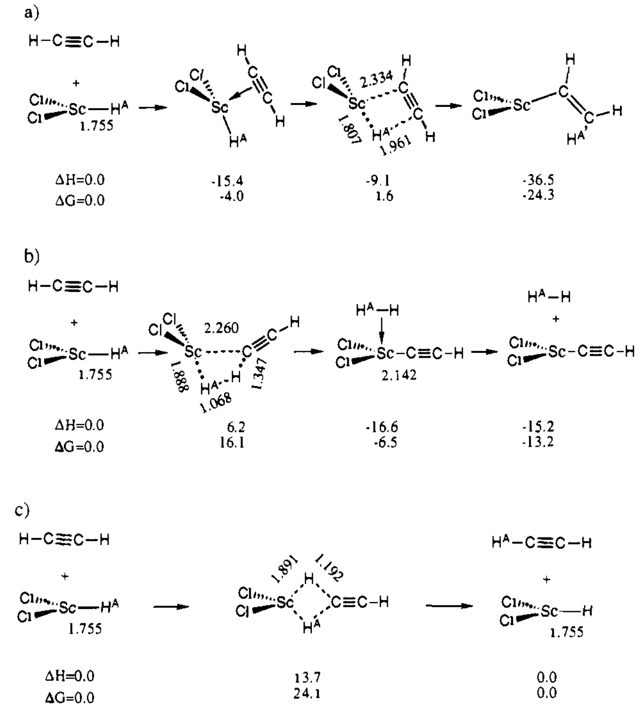

Figure 8. Potential energy profiles (in kcal/mol) at the CI level for reactions of acetylene with Cl_2ScH:[102] (a) insertion, (b) acetylide formation through σ-metathesis, and (c) H exchange through σ-metathesis.

Rappé and Goddard (RG) have studied the olefin metathesis catalytic cycle by the Cr, Mo, and W oxo complex.[103] RG have found that reaction 33 is exothermic by 20, 24, and 18 kcal/mol for the M = Cr, Mo, and W, respectively. While the bond between the transition metal and the oxide is a double bond in **63**, that in **64** is a triple bond which consists of two covalent π bonds and one σ donor–acceptor bond. The triple bond is stronger than the double bond by 31 and 23 kcal/mol for Cr and Mo, respectively and thus increases the exothermicity of reaction; the spectator oxo ligand plays an important role. This is consistent with the experimental fact that oxygen-containing compounds accelerate the metathesis and that a catalytic amount of oxygen is essential.[104] Since the σ bond in this triple bond is due to electron donation from oxygen to metal, RG have concluded that the high oxidation state of the metal and electron-withdrawing ligands are necessary.

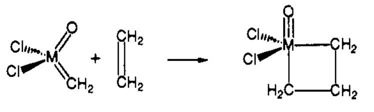

63 **64** (33)

Concerning catalytic olefin metathesis, the reverse reaction of reaction 33 has to take place, since metallacyclobutane is nothing but an intermediate. However, the reverse reaction is thermodynamically unfavorable. RG have estimated that Lewis acid and base stabilize the reactants of reaction 33 by 16 and 15 kcal/mol,

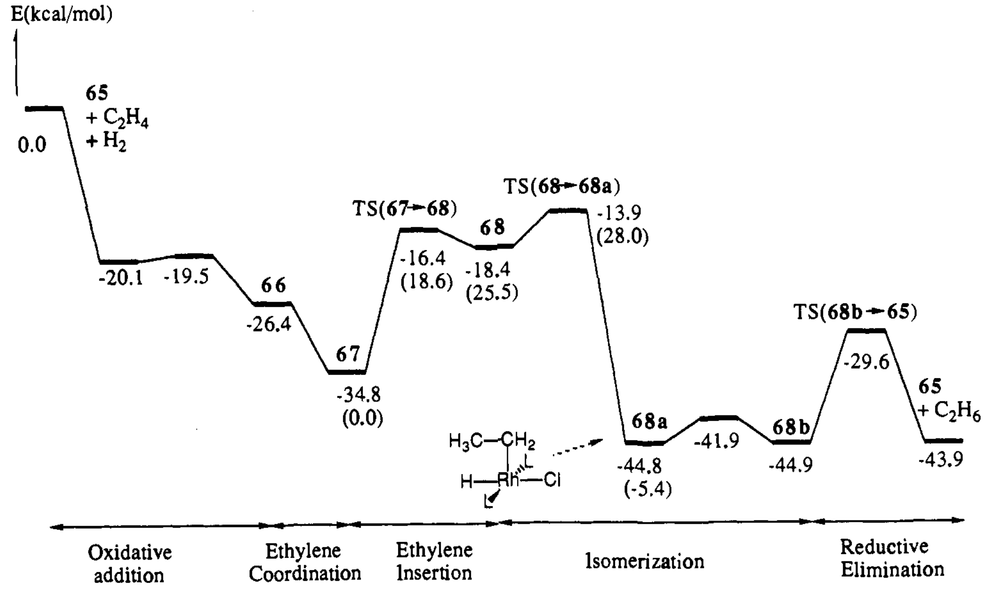

Figure 9. Potential energy profile of the entire catalytic cycle of the Halpern mechanism of olefin hydrogenation by the Wilkinson catalyst, in kcal/mol at the RHF-ECP level, relative to **65** + H_2 + C_2H_4. Numbers in parentheses are the MP2 energy at the RHF optimized structures, relative to **67**.[12]

SCHEME IV. Catalytic Cycle for Metathesis by W Oxo-Alkylidene Complex with Lewis Base (in kcal/mol)

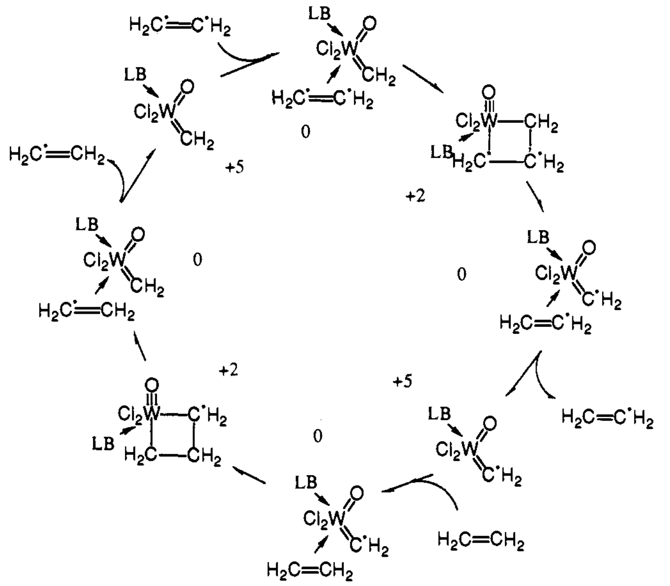

respectively, more than the products. Taking into account this effect, RG have proposed the energy profile of the catalytic cycle shown in Scheme IV for the tungsten catalyst. Although they have not searched for transition states and thus the kinetic factor has not been considered, the metathesis reaction of d^0 complex is expected to take place without a high activation energy as found in reaction 30. Therefore, the catalytic cycle shown in Scheme IV could proceed easily. RG have also found that in hydrocarbon oxidation by Cl_2MO_2 (M = Cr, Mo) (eq 34) the spectator oxo ligand plays an important role in stabilizing the intermediates.

$$Cl_2CrO_2 + C_2H_6 \rightarrow Cl_2CrO(OH)(C_2H_5) \rightarrow Cl_2CrO + C_2H_5OH \quad (34)$$

Dedieu and his co-workers[105] have studied the olefin hydrogenation catalytic cycle by the Wilkinson complex.[106] They have calculated the potential energy profile using experimental or assumed structures at the RHF level. As the authors have noted, reliable energetics of the elementary reactions including activation energies is required for complete discussion.

More recently, Daniel, Koga, Han, Fu, and Morokuma (DKHFM) have obtained the potential energy profile of this catalytic reaction by determining structures of the transition states as well as the intermediates for all the elementary steps by the ab initio energy gradient method.[12,107] The model catalytic cycle they have studied is shown in Scheme V. This cycle consists

SCHEME V

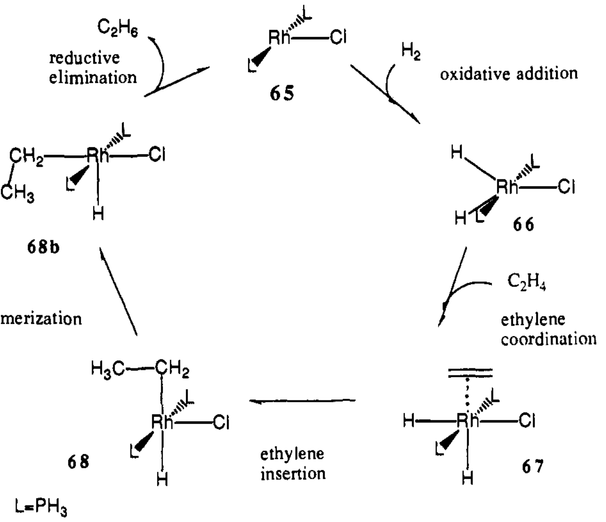

of (i) H_2 oxidative addition to the catalytic active intermediate, $RhClL_2$, (ii) olefin coordination, (iii) olefin insertion, (iv) isomerization of alkyl hydride complex, and (v) reductive elimination which produces alkane and regenerates the catalytic active intermediate, $RhClL_2$. This catalytic cycle was originally proposed by Halpern et al.,[23] although the isomerization of the alkyl hydride complex was not included in the original mechanism. In the actual calculation, ethylene and PH_3 were used in place of substituted ethylenes and triphenylphosphines in the real system. The energy profile obtained is shown in Figure 9.

SCHEME VI

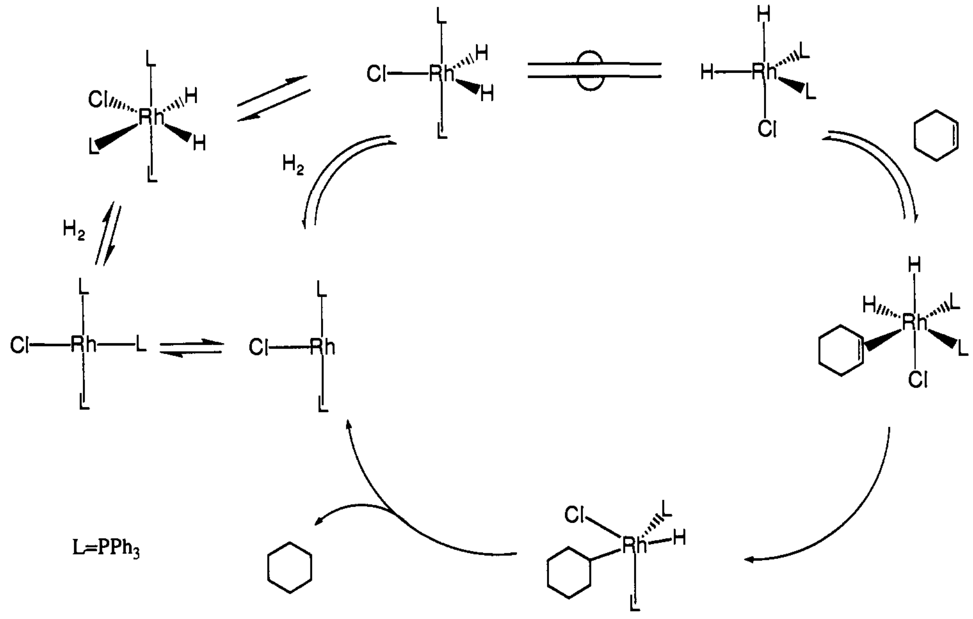

The first step of H_2 oxidative addition proceeds easily. The reactive intermediate $RhClL_2$ is coordinatively unsaturated and thus can easily activate a σ bond as discussed in section II.E. Following ethylene coordination, the endothermic ethylene insertion into the M–H bond takes place. This endothermicity was ascribed to the strong Rh–H bond in the reactant. The ligand trans to H is Cl, which has a weak trans influence, and thus the Rh–H bond to be broken is strong and furthermore the strongly electron-donating H and ethyl are trans to each other in the product; these factors result in large endothermicity and high activation energy. The following isomerization gives a more stable *cis*-ethyl hydride complex. The final step of reductive elimination takes place with a substantial activation energy.

The potential energy profile which DKHFM constructed from the energetics of these five elementary steps is smooth without excessive barriers and two stable intermediates, either of which would break the sequence of elementary reactions. Although this feature would be what is expected in any good catalyst, this study has provided the first theoretical demonstration that it actually is so in a model cycle.

DKHFM have found that the rate-determining step is olefin insertion combined with the first step of isomerization of the *trans*-ethyl hydride complex to the cis complex with an effective overall barrier height of 21 kcal/mol. DKHFM have considered that since the trans intermediate is in a shallow minimum, these two steps may take place as one combined step. The Halpern mechanism postulates that the rate-determining step is olefin insertion. Their theoretical study suggests that isomerization of the ethyl hydride complex as well as olefin insertion is an important component of the rate-determining step.

DKHFM have also discussed the effect of the transition metal and the ligand using model reactive intermediate, $RhH(PH_3)_2$, $Pt(PH_3)$, and $Pd(PH_3)$, as shown in Figure 10. In the reaction of $RhH(PH_3)_2$, in which the chloride of the Wilkinson catalyst was replaced by hydride, olefin insertion is almost thermoneutral, since the hydride weakens the Rh–H bond broken in the insertion. The hydride makes olefin insertion easier than that of the Wilkinson catalyst. In the cycle of $Pt(PH_3)$, olefin insertion requires a smaller activation energy as shown in section II.A. Although it seems that the barrier for olefin insertion step of $RhH(PH_3)_2$ and $Pt(PH_3)$ is so low that the catalytic cycle can proceed easily, one has to note that reverse β-hydride elimination can also take place with a low activation energy. These results have suggested that $RhH(PH_3)_2$ and $Pt(PH_3)$ are good catalysts for olefin isomerization rather than for olefin hydrogenation. On the other hand, the high activation energy for reverse β-hydride elimination of the Wilkinson catalyst prevents olefin isomerization. Chloride in the Wilkinson catalyst plays an important role in making the insertion rate determining. As expected from the difficulty of oxidative addition of the Pd complex discussed in section II.E, $Pd(PH_3)$ is not a good catalyst.

While two phosphines are always trans to each other in all the intermediates of the Halpern mechanism, Brown et al. have recently proposed a different mechanism on the basis of their molecular modeling calculations and NMR experiments. In their mechanism shown in Scheme VI *cis*-bisphosphine intermediates are active carriers of the catalytic cycle.[108] Bulky olefin is easier to coordinate to the cis intermediate than to the trans intermediate, since bulky phosphine such as triphenyl phosphine is trans to olefin. Koga and Morokuma have compared this Brown mechanism with the Halpern mechanism.[107] In Figure 11 is shown the potential energy profile they calculated for the Brown mechanism.

The first point of difference of the Brown mechanism from the Halpern mechanism is isomerization of $H_2RhCl(PR_3)_2$. They have determined the structure of **66b**, the intermediate of the Brown mechanism, which has the vacant coordination site trans to one of the phosphines and thus receives the coordination of the bulky olefin. Isomerization of **66** → **66b** is 21 kcal/mol endothermic and requires a large activation energy of 27 kcal/mol. Therefore, isomerization to the cis in-

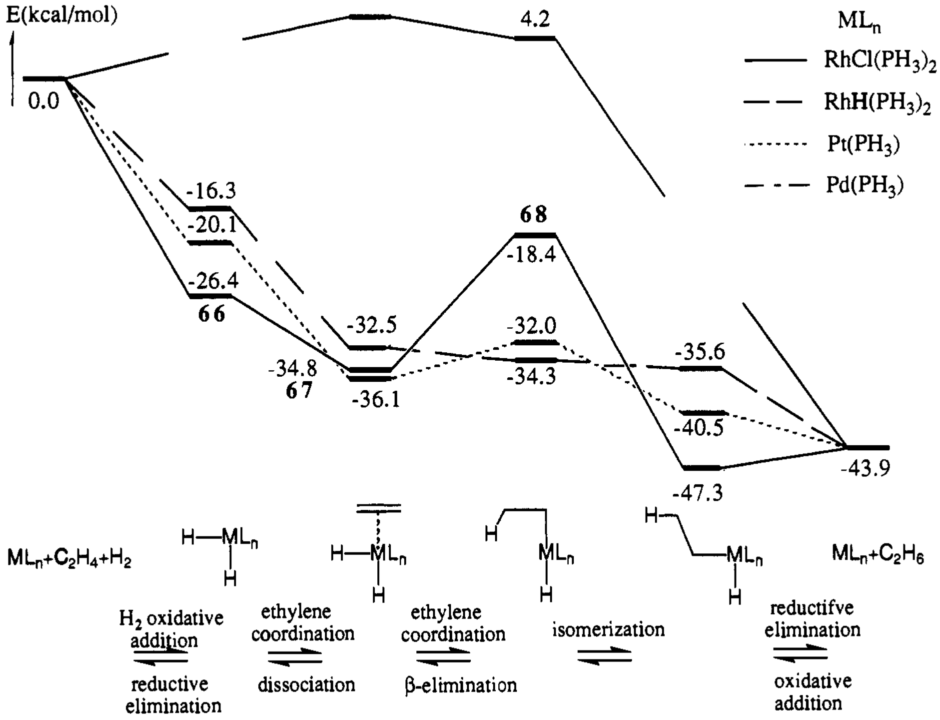

Figure 10. Energy changes (in kcal/mol) of the full hydrogenation cycle by $RhCl(PH_3)_2$, $RhH(PH_3)_2$, $Pd(PH_3)$, and $Pt(PH_3)$. The profiles show only the energies of intermediates but not those of transition states connecting them.[12]

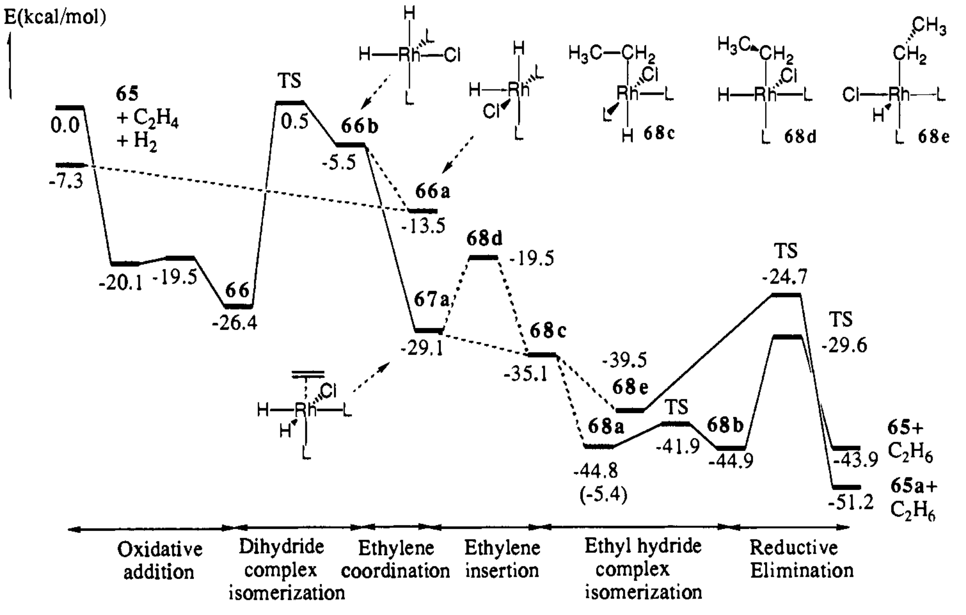

Figure 11. Potential energy profile of the catalytic cycle of the Brown mechanism of olefin hydrogenation by the Wilkinson catalyst, in kcal/mol at the RHF-ECP level, relative to **65** + H_2 + C_2H_4.[107]

termediate is not an easy process.

The remaining steps, ethylene insertion and isomerization of the ethyl hydride complex, do not require large activation energies. Thus, the exothermic ethylene insertion in **67a**, the result of ethylene coordination to **66b**, takes place easily to give **68c**. Isomerization of **68c** gives **68a**, the trans intermediate in the Halpern mechanism, through PH_3 migration or **68e** through Cl migration. Reductive elimination of **68e** giving **65a** requires the substantial activation energy of 15 kcal/mol, which is comparable with the activation energy for reductive elimination of **68a**.

There are two possibilities in the reactions of **65a**. The first is that **65a** isomerizes to **65** due to the steric repulsion between two phosphines and that the same reaction path **65** → **66** → **66b** is followed. The second possibility is that H_2 oxidative addition to **65a** takes place to give directly **66a** and thus in the subsequent catalytic cycles intermediates always have *cis*-phosphines. In this case coordination of bulky olefin to **66a** is prohibited because of the steric repulsion between the olefin and two bulky phosphines cis to the olefin. Thus **66a** → **66b** isomerization has to take place before the catalytic cycle proceeds.

Their potential energy profile shows that in the Brown mechanism, setting aside the high energy required for isomerization from **66** to **66b**, the final step of the reductive elimination would require the highest activation energy and that olefin insertion, the rate-determining step in the Halpern mechanism, is an easy process. Therefore, they have concluded that in the cases in which olefin insertion has been found to be rate determining, the Halpern mechanism is clearly more consistent and acceptable. Since olefin and phosphine used in these calculations are not bulky, they have not ruled out the possibility of the cis mechanism. They have discussed the reaction path when olefin and phosphine are bulky, to show that the cis mechanism may become possible if the trans to cis isomerization can take place through, for instance, ligand exchange, although it would exhibit kinetics quite different from that of the Halpern mechanism.

Recently, Ding, Koga, and Morokuma have studied the full catalytic cycle of hydroformylation by the Rh catalyst (Scheme VII).[109] Although H_2 oxidative addition is believed to be a rate-determining step,[1] the activation energy of this step has been calculated to be 1.4 kcal/mol at the MP2 level. While ethylene insertion and carbonyl insertion requires much larger activation energy of about 20 kcal/mol, propionaldehyde dissociation, the final step, is very endothermic (31.5 kcal/mol).

SCHEME VII

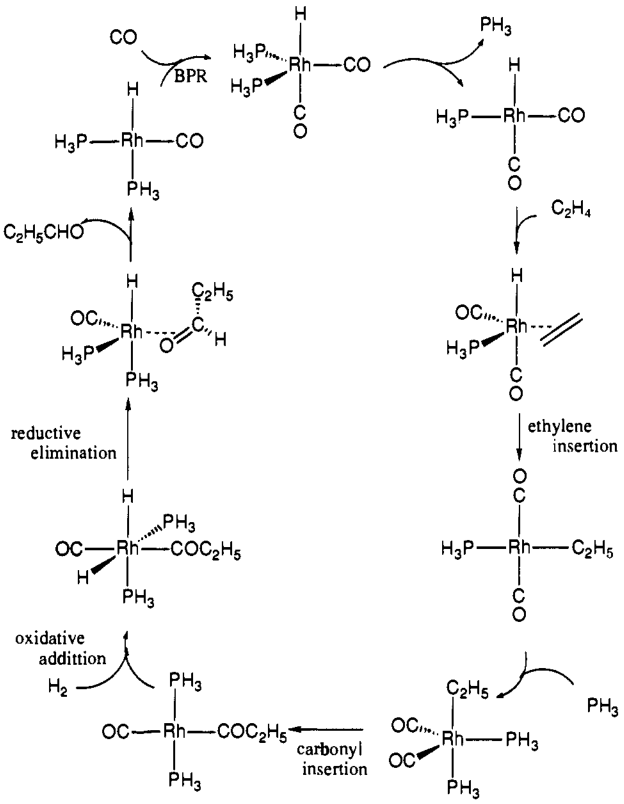

IV. Concluding Remarks

In this article we reviewed ab initio MO studies of elementary catalytic reactions and catalytic cycles. These studies have demonstrated that ab initio MO calculations, specially with the energy gradient method, could give valuable insight into catalytic reactions by transition-metal complexes. By determining structures of a reactant, a product, and a transition state, the reaction path could be elucidated. Thus, the ab initio MO calculations can give more quantitative information than the orbital symmetry arguments. For instance, the symmetry-allowed H_2 oxidative addition to $Pt(PH_3)_2$ has been shown to have a small but significant activation barrier. In addition, by changing the transition metal, ligands, and substituents, their effects on the potential energy surface could be explored more quantitatively. For instance, compared with Pt, Pd disfavors oxidative addition because of its d^{10} atomic ground state, whereas it favors carbonyl insertion because of the weaker Pd–ligand bond. It is expected that ab initio MO calculations will make ever increasing contribution to better understanding and hopefully for designing catalytic reactions of transition-metal complexes.

The theoretical calculations as reviewed here, however, are still in an early stage of development. There are many aspects to be improved. For instance, catalytic reactions are carried out in solution. The effect of solvent has to be elucidated. In some case, solvent would play a role of additional ligand as well as a general acid or base. Phosphines in experiment are usually not PH_3 but bulkier phosphines such as trialkyl- and triphenylphosphine. The steric effect as well as the electronic effect of such substituents has to be properly taken into account.

From computational methodological point of view, there are several points to which comments should be made. For a complex of bare transition metal atom or ion, such as $NiCH_2$, there are several low-lying electronic states originating from various atomic configurations, such as d^8s^2, d^9s, and d^{10}. In order to take into account these electronic configurations correctly, one has to use multiconfiguration wave functions that can handle near-degeneracy effect or nondynamical electron correlation. Transition-metal complexes discussed in this review, on the other hand, have several strong ligands, which stabilize mostly the configuration with the largest number of d electrons. Consequently, the single configuration description is a good approximation for geometry determination. However, in several notable exceptions, the dynamic electron correlation can make a large difference in optimized geometries. One such example is the geometry of the transition state for C–H activation.[89] In another example, the HF bond distances for M–CO, M–C_2H_4, and M–Cp bonds for Fe, Co, and Ni tend to be too long; the details will be discussed by Veillard in this issue.[110]

In order to obtain a reliable energetics, it is necessary to take into account the electron correlation effect, even if the single determinantal wave function is a good starting point. As seen in the C–H activation by $RhCl(PH_3)_2$, when a metal–R bond is covalent with a large d character, the energetics of reaction is drastically changed by electron correlation. On the other hand, when the metal–R bond is ionic, the effect is small. A latter example is H_2 oxidative addition to $Pt(PH_3)_2$. In either case the energy of this dynamic electron correlation can be obtained by the single reference SDCI or the Møller–Plesset perturbation theory, when the single determinant can represent the electronic structure qualitatively. The latter method is cheaper and thus is often used. When the nondynamical electron correlation is important, as in complexes of bare metals and metal ions, multireference methods such as the MRSDCI have to be used.

V. References

(1) See, for instance: (a) Collman, J. P.; Hegedus, L. S.; Norton, J. R.; Finke, R. G. *Principles and Applications of Organo-*

transition Metal Chemistry; University Science Books: Mill Valley, CA, 1987. (b) Cotton, F. A.; Wilkinson, G. *Advanced Inorganic Chemistry*; Wiley: New York, 1988. (c) Yamamoto, A. *Organotransition Metal Chemistry*; Wiley: New York, 1986.

(2) (a) Dedieu, A. In *Topics in Physical Organometallic Chemistry*; Gielen, M. F. Ed.; Freund Publishing House: London, 1985; Vol. 1, p 1. (b) Koga, N.; Morokuma, K. In *Topics in Physical Organometallic Chemistry*; Gielen, M. F. Ed.; Freund Publishing House: London, 1989; Vol. 3, p 1.

(3) For example: Hoffmann, R. *J. Chem. Phys.* **1963**, *39*, 1397.

(4) Albright, T. A.; Burdett, J. K.; Whangbo, M.-H. *Orbital Interactions in Chemistry*; Wiley: New York, 1985.

(5) (a) Hehre, W. J.; Radom, L.; Schleyer, P. v. R.; Pople, J. A. *Ab Initio Molecular Orbital Theory*; Wiley: New York, 1986. (b) *Quantum Chemistry Literature Data Base*; Ohno, K., Morokuma, K., Eds.; Elsevier: Amsterdam, 1982; *J. Mol. Struct.* (*THEOCHEM*) **1982**, *91* (Supplement 1), 1; *J. Mol. Struct.* (*THEOCHEM*) **1983**, *106* (Supplement 2), 1; *J. Mol. Struct.* (*THEOCHEM*) **1984**, *119* (Supplement 3), 1; *J. Mol. Struct.* (*THEOCHEM*) **1985**, *134* (Supplement 4), 1; *J. Mol. Struct.* (*THEOCHEM*) **1986**, *148* (Supplement 5), 1; *J. Mol. Struct.* (*THEOCHEM*) **1987**, *154* (Supplement 6), 1; *J. Mol. Struct.* (*THEOCHEM*) **1988**, *182* (Supplement 7), 1; *J. Mol. Struct.* (*THEOCHEM*) **1989**, *203* (Supplement 8), 1; *J. Mol. Struct.* (*THEOCHEM*) **1990**, *211* (Supplement 9), 1.

(6) (a) Hay, P. J.; Wadt, W. R. *J. Chem. Phys.* **1985**, *82*, 270. (b) Wadt, W. R.; Hay, P. J. *J. Chem. Phys.* **1985**, *82*, 284. (c) Hay, P. J.; Wadt, W. R. *J. Chem. Phys.* **1985**, *82*, 299.

(7) Sakai, Y.; Miyoshi, E.; Klobukowski, M.; Huzinaga, S. *J. Comput. Chem.* **1987**, *8*, 226; 256.

(8) (a) Pyykkö, P.; Desclaux, J.-P. *Acc. Chem. Res.* **1979**, *12*, 276. (b) Pyykkö, P. *Chem. Rev.* **1988**, *88*, 563.

(9) (a) Versluis, L.; Ziegler, T.; Fan, L. *Inorg. Chem.* **1990**, *29*, 5340. (b) Versluis, L.; Ziegler, T. *J. Am. Chem. Soc.* **1990**, *112*, 6763. (c) Versluis, L.; Ziegler, T.; Baerends, J.; Ravenek, W. *J. Am. Chem. Soc.* **1989**, *111*, 2018. (d) Ziegler, T.; Versluis, L.; Tschinke, V. *J. Am. Chem. Soc.* **1986**, *108*, 612. (e) Versluis, L.; Ziegler, T. *Organometallics* **1990**, *9*, 2985. (f) Ziegler, T.; Fan, L.; Tschinke, V.; Becke, A. *J. Am. Chem. Soc.* **1989**, *111*, 2018. (g) Harrod, J. F.; Ziegler, T.; Tschinke, V. *Organometallics* **1990**, *9*, 897.

(10) Ziegler, T. *Chem. Rev.* **1991**, *91*, 651 (in this issue).

(11) (a) Koga, N.; Kitaura, K.; Obara, S.; Morokuma, K. *J. Am. Chem. Soc.* **1985**, *107*, 7109. (b) Koga, N.; Morokuma, K. In *Quantum Chemistry*: *The Challenge of Transition Metals and Coordination Chemistry*; Veillard, A. Ed.; NATO ASI series 176: Reidel: Dordrecht, 1986; p 351.

(12) (a) Koga, N.; Daniel, C.; Han, J.; Fu, X. Y.; Morokuma, K. *J. Am. Chem. Soc.* **1987**, *109*, 3455. (b) Daniel, C.; Koga, N.; Han, J.; Fu, X. Y.; Morokuma, K. *J. Am. Chem. Soc.* **1988**, *110*, 3773.

(13) Koga, N.; Jin, S.-Q.; Morokuma, K. *J. Am. Chem. Soc.* **1988**, *110*, 3417.

(14) (a) Møller, C.; Plessett, M. S. *Phys. Rev.* **1934**, *46*, 618. (b) Binkley, J. S.; Pople, J. A. *Int. J. Quantum Chem.* **1975**, *9*, 229.

(15) Thorn, D. L.; Hoffmann, R. *J. Am. Chem. Soc.* **1978**, *100*, 2079.

(16) Sakaki, S.; Kato, H.; Kanai, H.; Tarama, K. *Bull. Chem. Soc. Jpn.* **1975**, *48*, 813.

(17) Fukui, K.; Inagaki, S. *J. Am. Chem. Soc.* **1975**, *97*, 4445.

(18) Tatsumi, K.; Yamaguchi, K.; Fueno, T. *J. Mol. Catal.* **1977**, *2*, 437.

(19) Bäckvall, J.-E.; Björkman, E. E.; Pettersson, L.; Siegbahn, P. *J. Am. Chem. Soc.* **1984**, *106*, 4369.

(20) (a) Brookhart, M.; Green, M. L. H. *J. Organomet. Chem.* **1983**, *250*, 395. (b) Brookhart, M.; Green, M. L. H.; Wong, L.-T. *Prog. Inorg. Chem.* **1988**, *36*, 1.

(21) (a) Koga, N.; Obara, S.; Morokuma, K. *J. Am. Chem. Soc.* **1984**, *106*, 625. (b) Obara, S.; Koga, N.; Morokuma, K. *J. Organomet. Chem.* **1984**, *270*, C33. (c) Koga, N.; Morokuma, K. *J. Am. Chem. Soc.* **1988**, *110*, 108.

(22) Cotton, F. A.; LaCour, T.; Stanislowski, G. *J. Am. Chem. Soc.* **1974**, *96*, 734.

(23) (a) Halpern, J.; Wong, C. S. *J. Chem. Soc., Chem. Commun.* **1973**, 629. (b) Halpern, J. In *Organotransition Metal Chemistry*; Ishii, Y., Tsutsui, M. Eds.; Plenum: New York, 1975; p 109. (c) Halpern, J.; Okamoto, T.; Zakhariev, A. *J. Mol. Catal.* **1976**, *2*, 65.

(24) (a) Ugi, I.; Marquarding, D.; Klusacek, H.; Gillespie, P. *Acc. Chem. Res.* **1971**, *4*, 288. (b) Holmes, R. R. *Acc. Chem. Res.* **1972**, *5*, 296. (c) Berry, R. S. *J. Chem. Phys.* **1960**, *32*, 933. (d) Muetterties, E. L. *J. Am. Chem. Soc.* **1969**, *91*, 1636, 4115. (e) Ugi, I.; Ramirez, F.; Marquarding, D.; Klusacek, H.; Gokel, G.; Gillespie, P. *Angew. Chem., Int. Ed. Engl.* **1970**, *9*, 725.

(25) Rossi, A. R.; Hoffmann, R. *Inorg. Chem.* **1975**, *14*, 365.

(26) (a) Antolovic, D.; Davidson, E. R. *J. Am. Chem. Soc.* **1987**, *109*, 977. (b) Antolovic, D.; Davidson, E. R. *J. Am. Chem. Soc.* **1987**, *109*, 5828.

(27) Versluis, L. Ph.D. Thesis, The University of Calgary, 1989.

(28) Novaro, O.; Blaisten-Barojas, E.; Clementi, E.; Giunchi, G.; Ruiz-Vizcaya, M. E. *J. Chem. Phys.* **1978**, *68*, 2337.

(29) Fujimoto, H.; Yamasaki, T.; Mizutani, H.; Koga, N. *J. Am. Chem. Soc.* **1985**, *107*, 6157.

(30) Jolly, C. A.; Marynick, D. S. *J. Am. Chem. Soc.* **1989**, *111*, 7968.

(31) (a) Kawamura, H.; Koga, N.; Morokuma, K. *Abstracts*. 36th Symposium on Organometallic Chemistry, Tokyo, Japan, September 1989; Kinki Chemical Society: Osaka, 1989; Paper PA114. (b) Kawamura-Kuribayashi, H.; Koga, N.; Morokuma, K., submitted.

(32) (a) Herrmann, W. A. *Angew. Chem., Int. Ed. Engl.* **1982**, *21*, 117. (b) Blackborow, J. R.; Daroda, R. J.; Wilkinson, G. *Coord. Chem. Rev.* **1982**, *43*, 17.

(33) (a) Grimett, D. L.; Labinger, J. A.; Bonfiglio, J. N.; Masuo, S. T.; Shearin, E.; Miller, J. S. *Organometallics* **1983**, *2*, 1325. (b) Masters, C. *Adv. Organomet. Chem.* **1979**, *17*, 61. (c) Fahey, D. R. *J. Am. Chem. Soc.* **1981**, *103*, 136.

(34) Moloy, K. G.; Marks, T. J. *J. Am. Chem. Soc.* **1984**, *106*, 7051.

(35) (a) See: ref 1a, p 369. (b) Connor, J. A.; Zafarani-Moattar, M. T.; Bickerton, J.; El Saied, N. I.; Suradi, S.; Carson, R.; Al Takhin, G.; Skinner, H. A. *Organometallics* **1982**, *1*, 1166. (c) Lane, K. L.; Sallans, L.; Squires, R. R. *Organometallics* **1984**, *4*, 408.

(36) Sakaki, S.; Kitaura, K.; Morokuma, K.; Ohkubo, K. *J. Am. Chem. Soc.* **1983**, *105*, 2280.

(37) (a) Koga, N.; Morokuma, K. *J. Am. Chem. Soc.* **1985**, *107*, 7230. (b) Koga, N.; Morokuma, K. *J. Am. Chem. Soc.* **1986**, *108*, 6536.

(38) (a) Nakamura, S.; Dedieu, A. *Chem. Phys. Lett.* **1984**, *111*, 243. (b) Dedieu, A.; Nakamura, S. In *Quantum Chemistry*: *The Challenge of Transition Metals and Coordination Chemistry*; Veillard, A., Ed.; NATO ASI series 176; Reidel: Dordrecht, 1986; p 277.

(39) Berke, H.; Hoffmann, R. *J. Am. Chem. Soc.* **1978**, *100*, 7224.

(40) (a) Axe, F. U.; Marynick, D. S. *J. Am. Chem. Soc.* **1988**, *110*, 3728. (b) Axe, F. U.; Marynick, D. S. *Organometallics* **1987**, *6*, 572.

(41) Fujimoto, H.; Koga, N.; Fukui, K. *J. Am. Chem. Soc.* **1981**, *103*, 7452.

(42) (a) Coffield, T. H.; Kozikowski, J.; Closson, R. D. *J. Org. Chem.* **1957**, *22*, 598. (b) Calderazzo, F.; Cotton, F. A. *Inorg. Chem.* **1962**, *1*, 30. (c) Keblys, K. A.; Filbey, A. H. *J. Am. Chem. Soc.* **1960**, *82*, 4204. (d) Mawby, R. J.; Basolo, F.; Pearson, G. *J. Am. Chem. Soc.* **1964**, *86*, 3994. (e) Calderazzo, F.; Noack, K. *Coord. Chem. Rev.* **1966**, *1*, 118. (f) Noack, K.; Calderazzo, F. *J. Organomet. Chem.* **1967**, *10*, 101. (g) Cawse, J. N.; Fiato, R. A.; Pruett, R. L. *J. Organomet. Chem.* **1979**, *172*, 405. (h) McHugh, T. M.; Rest, A. J. *J. Chem. Soc., Dalton Trans.* **1980**, 2323. (i) Flood, T. C.; Jensen, J. E.; Statler, J. A. *J. Am. Chem. Soc.* **1981**, *103*, 4410.

(43) Ziegler, T.; Versluis, L.; Tschinke, V. *J. Am. Chem. Soc.* **1986**, *108*, 612.

(44) See, for instance: Shavitt, I. In *Methods of Electronic Structure Theory*; Plenum: New York, 1977; p 189.

(45) (a) Siegbahn, P. E. M.; Almlöf, J.; Heiberg, A.; Roos, B. O. *J. Chem. Phys.* **1981**, *74*, 2384. (b) Roos, B. O.; Taylor, P. R.; Siegbahn, P. E. M. *Chem. Phys.* **1980**, *48*, 157.

(46) Dedieu, A.; Sakaki, S.; Strich, A.; Siegbahn, P. E. M. *Chem. Phys. Lett.* **1987**, *133*, 317.

(47) Axe, F. U.; Marynick, D. S. *Chem. Phys. Lett.* **1987**, *141*, 455.

(48) Dedieu, A. In *The Challenge of d and f Electrons*: *Theory and Computation*; Salahub, D. R., Zerner, M. C. Eds.; American Chemical Society symposium series 394; American Chemical Society: Washington, DC, 1989; p 58.

(49) Koga, N.; Morokuma, K. *New. J. Chem.*, in press.

(50) Beck, R. F.; Breslow, D. S. *J. Am. Chem. Soc.* **1961**, *83*, 4023.

(51) Antolovic, D.; Davidson, E. R. *J. Chem. Phys.* **1988**, *88*, 4967.

(52) Luthi, H. P.; Siegbahn, P. E. M.; Almlöf, J. *J. Phys. Chem.* **1985**, *89*, 2156.

(53) Rappé, A. K. *J. Am. Chem. Soc.* **1987**, *109*, 5605.

(54) Bobrowicz, F. W.; Goddard, W. A. In *Methods of Electronic Structure Theory*; Plenum: New York, 1977; p 79.

(55) Curtis, M. D.; Shiu, K.-B.; Butler, W. M. *J. Am. Chem. Soc.* **1986**, *108*, 1550.

(56) McKee, M. L.; Dai, C. H.; Worley, S. D. *J. Phys. Chem.* **1988**, *92*, 1056.

(57) (a) Worley, S. D.; Mattson, G. A.; Caudill, R. *J. Phys. Chem.* **1983**, *87*, 1671. (b) Day, C. H.; Worley, S. D. *J. Phys. Chem.* **1986**, *90*, 4219. (c) Henderson, M. A.; Worley, S. D. *J. Phys. Chem.* **1985**, *89*, 392, 1417.

(58) Yates, J. T.; Cavanagh, R. R. *J. Catal.* **1982**, *74*, 97.

(59) Pacchioni, G.; Fantucci, P.; Koutecky, J.; Ponec, V. *J. Catal.* **1988**, *112*, 34.

(60) (a) van der Lee, G.; Schuller, B. H.; Favre, T. L. F.; Post, H.; Ponec, V. *J. Catal.* **1986**, *98*, 522. (b) van der Lee, G.; Ponec, V. *J. Catal.* **1986**, *98*, 511.

(61) Dombek, B. D. *Adv. Catal.* **1983**, *32*, 325.
(62) Nakamura, S.; Morokuma, K. *Abstracts*, 33rd Symposium on Organometallic Chemistry, Tokyo, Japan, October, 1986; Kinki Chemical Society: Osaka, 1986; Paper A109.
(63) (a) Darenbourg, D. J.; Kudaroski, R. A. *Adv. Organomet. Chem.* **1983**, *22*, 129. (b) Palmer, D. A.; Van Eldik, R. *Chem. Rev.* **1983**, *83*, 651. (c) Walther, D. *Coord. Chem. Rev.* **1987**, *79*, 135. (d) Braustein, P.; Matt, D. *Chem. Rev.* **1988**, *88*, 747.
(64) Bo, C.; Dedieu, A. *Inorg. Chem.* **1989**, *28*, 304.
(65) Sakaki, S.; Ohkubo, K. *Inorg. Chem.* **1988**, *27*, 2020; **1989**, *28*, 2583.
(66) Canestrani, M.; Green, M. L. *J. Chem. Soc., Dalton Trans.* **1982**, 1789.
(67) Carter, E. A.; Goddard, W. A. *J. Am. Chem. Soc.* **1987**, *109*, 579.
(68) Sakaki, S.; Nishikawa, M.; Ohyoshi, A. *J. Am. Chem. Soc.* **1980**, *102*, 4062.
(69) Eisenstein, O.; Hoffmann, R. *J. Am. Chem. Soc.* **1980**, *102*, 6148.
(70) (a) Nakamura, S.; Dedieu, A. *Theor. Chim. Acta* **1982**, *61*, 587. (b) Dedieu, A.; Nakamura, S. *Nouv. J. Chimie* **1984**, *8*, 317.
(71) Fujimoto, H.; Yamasaki, T. *J. Am. Chem. Soc.* **1986**, *108*, 578.
(72) (a) Sakaki, S.; Maruta, K.; Ohkubo, K. *Inorg. Chem.* **1987**, *26*, 2499. (b) Sakaki, S.; Maruta, K.; Ohkubo, K. *J. Chem. Soc., Dalton Trans.* **1987**, 361.
(73) (a) Nakatsuji, H.; Ushio, J.; Han, J.; Yonezawa, T. *J. Am. Chem. Soc.* **1983**, *105*, 426. (b) Ushio, J.; Nakatsuji, H.; Yonezawa, T. *J. Am. Chem. Soc.* **1984**, *106*, 5892.
(74) Yoshida, T.; Yamagata, T.; Tulip, T. H.; Ibers, J. A.; Otsuka, S. *J. Am. Chem. Soc.* **1978**, *100*, 2623.
(75) (a) Kitaura, K.; Obara, S.; Morokuma, K. *J. Am. Chem. Soc.* **1981**, *103*, 2891. (b) Obara, S.; Kitaura, K.; Morokuma, K. *J. Am. Chem. Soc.* **1984**, *106*, 7482.
(76) Noell, J. O.; Hay, P. J. *J. Am. Chem. Soc.* **1982**, *104*, 4578.
(77) Low, J. J.; Goddard, W. A. *J. Am. Chem. Soc.* **1984**, *106*, 6928.
(78) (a) Packett, D. L.; Trogler, W. C. *J. Am. Chem. Soc.* **1986**, *108*, 5036. (b) Packett, D. L.; Jensen, C. M.; Cowan, R. L.; Strouse, C. E.; Trogler, W. C. *Inorg. Chem.* **1985**, *24*, 3578.
(79) (a) Blomberg, M. R. A.; Siegbahn, P. E. M. *J. Chem. Phys.* **1983**, *78*, 986. (b) Blomberg, M. R. A.; Siegbahn, P. E. M. *J. Chem. Phys.* **1983**, *78*, 5682.
(80) Brandemark, U. B.; Blomberg, M. R. A.; Pettersson, L. G. M.; Siegbahn, P. E. M. *J. Phys. Chem.* **1984**, *88*, 4617.
(81) (a) Low, J. J.; Goddard, W. A. *J. Am. Chem. Soc.* **1984**, *106*, 8321. (b) Low, J. J.; Goddard, W. A. *Organometallics* **1986**, *5*, 609. (c) Low, J. J.; Goddard, W. A. *J. Am. Chem. Soc.* **1986**, *108*, 6115.
(82) Blomberg, M. R. A.; Siegbahn, P. E. M.; Bäckvall, J.-E. *J. Am. Chem. Soc.* **1987**, *109*, 4450.
(83) Kubas, G. J.; Ryan, R. R.; Swanson, B. I.; Vergamini, P. J.; Wasserman, H. J. *J. Am. Chem. Soc.* **1984**, *106*, 451.
(84) Kubas, G. J. *Acc. Chem. Res.* **1988**, *21*, 120.
(85) Hay, P. J. *J. Am. Chem. Soc.* **1987**, *109*, 705.
(86) Blomberg, M. R. A.; Brandemark, U.; Siegbahn, P. E. M. *J. Am. Chem. Soc.* **1983**, *105*, 5557.
(87) Koga, N.; Morokuma, K. *Organometallics* **1991**, *10*, 946.
(88) (a) Shilov, A. E. *Activation of Saturated Hydrocarbons*; Reidel: Dordrecht, 1984. (b) Crabtree, R. H. *Chem. Rev.* **1985**, *85*, 245. (c) Crabtree, R. H. *Acc. Chem. Res.* **1990**, *23*, 95.
(89) Koga, N.; Morokuma, K. *J. Phys. Chem.* **1990**, *94*, 5454.
(90) Sakakura, T.; Sodeyama, T.; Sasaki, K.; Wada, K.; Tanaka, M. *J. Am. Chem. Soc.* **1990**, *112*, 7221.
(91) (a) Elkind, J. L.; Armentrout, P. B. *J. Phys. Chem.* **1987**, *91*, 2037. (b) Armentrout, P. B.; Beauchamp, J. L. *Acc. Chem. Res.* **1989**, *22*, 315. (c) Schwarz, H. *Acc. Chem. Res.* **1989**, *22*, 282.
(92) (a) Balasubramanian, K. *Chem. Phys. Lett.* **1987**, *135*, 288. (b) Balasubramanian, K. *J. Chem. Phys.* **1987**, *87*, 2800. (c) Balasubramanian, K.; Feng, P. Y.; Liao, M. Z. *J. Chem. Phys.* **1988**, *88*, 6955. (d) Balasubramanian, K.; Ravimohan, Ch. *Chem. Phys. Lett.* **1988**, *145*, 39. (e) Balasubramanian, K.; Liao, M. Z. *J. Chem. Phys.* **1988**, *92*, 361. (f) Balasubramanian, K.; Liao, M. Z. *J. Phys. Chem.* **1989**, *93*, 89. (g) Balasubramanian, K.; Ravimohan, Ch. *J. Phys. Chem.* **1989**, *93*, 4490. (h) Das, K. K.; Balasubramanian, K. *J. Chem. Phys.* **1990**, *92*, 6697.
(93) (a) Novaro, O.; García-Prieto, J.; Poulain, E.; Ruiz, M. E. *J. Mol. Struct.* (*THEOCHEM*) **1986**, *135*, 79. (b) Jarque, C.; Novaro, O.; Ruiz, M. E.; García-Prieto, J. *J. Am. Chem. Soc.* **1986**, *108*, 3507.
(94) (a) Nakatsuji, H.; Hada, M.; Yonezawa, T. *J. Am. Chem. Soc.* **1987**, *109*, 1902. (b) Nakatsuji, H.; Hada, M.; Yonezawa, T. *Surface Sci.* **1987**, *185*, 319. (c) Nakatsuji, H.; Matsuzaki, Y.; Yonezawa, T. *J. Chem. Phys.* **1988**, *88*, 5759.
(95) Upton, T. H.; Rappé, A. K. *J. Am. Chem. Soc.* **1985**, *107*, 1206.
(96) (a) Lee, J. B.; Ott, K. C.; Grubbs, R. H. *J. Am. Chem. Soc.* **1982**, *104*, 7491. (b) Straus, D. A.; Grubbs, R. H. *Organometallics* **1982**, *1*, 1658.
(97) Tolbert, M. A.; Beauchamp, J. L. *J. Am. Chem. Soc.* **1984**, *106*, 8117.
(98) (a) Jeske, G.; Lauke, H.; Mauermann, H.; Swepston, P. N.; Schumann, H.; Marks, T. J. *J. Am. Chem. Soc.* **1985**, *107*, 8091. (b) Jeske, G.; Lauke, H.; Mauermann, H.; Schumann, H.; Marks, T. J. *J. Am. Chem. Soc.* **1985**, *107*, 8111.
(99) Thompson, M. E.; Baxter, S. M.; Bulls, A. R.; Burger, B. J.; Nolan, M. C.; Santarsiero, B. D.; Schaefer, W. P.; Bercaw, J. E. *J. Am. Chem. Soc.* **1987**, *109*, 203.
(100) Christ, C. S.; Eyler, J. R.; Richardson, D. E. *J. Am. Chem. Soc.* **1990**, *112*, 596.
(101) Steigerwald, M. L.; Goddard, W. A. *J. Am. Chem. Soc.* **1984**, *106*, 308.
(102) Rappé, A. K. *Organometallics* **1990**, *9*, 466. See, also: Rappé, A. K. *Organometallics* **1987**, *6*, 354.
(103) (a) Rappé, A. K.; Goddard, W. A. *J. Am. Chem. Soc.* **1982**, *104*, 448. (b) Rappé, A. K.; Goddard, W. A. *J. Am. Chem. Soc.* **1982**, *104*, 3287.
(104) (a) Basset, J. M.; Coudurier, G.; Mutim, R.; Proliaud, H.; Trambouze, Y. *J. Catal.* **1974**, *34*, 196. (b) Mocella, M. T.; Rovner, R.; Muetterties, E. L. *J. Am. Chem. Soc.* **1976**, *98*, 1689.
(105) (a) Dedieu, A. *Inorg. Chem.* **1980**, *19*, 375. (b) Dedieu, A.; Hyla-Krypsin, I. *J. Organomet. Chem.* **1981**, *220*, 115. (c) Dedieu, A.; Strich, A. *Inorg. Chem.* **1979**, *18*, 2943. (d) Dedieu, A. *Inorg. Chem.* **1981**, *20*, 2803.
(106) (a) Osborn, J. A.; Jardine, F. H.; Young, J. F.; Wilkinson, G. *J. Chem. Soc. A* **1966**, 1711. (b) Jardine, F. H.; Osborn, J. A.; Wilkinson, G. *J. Chem. Soc. A* **1967**, 1574. (c) Montelatici, S.; van der Ent, A.; Osborn, J. A.; Wilkinson, G. *J. Chem. Soc. A* **1968**, 1054.
(107) Koga, N.; Morokuma, K. In *The Challenge of d and f Electrons Theory and Computation*; Salahub, D. R., Zerner, M. C., Eds.; American Chemical Society symposium series 394; American Chemical Society: Washington, DC, 1989; p 77.
(108) Brown, J. M.; Evans, P. L.; Lucy, A. R. *J. Chem. Soc., Perkin Trans. 2* **1987**, 1589.
(109) Ding, Y. B.; Koga, N.; Morokuma, K. *Abstracts*, 37th Symposium on Organometallic Chemistry, Osaka, Japan, October 1990; Kinki Chemical Society: Osaka, 1990; Paper PA106.
(110) Veillard, A. *Chem. Rev.* **1991**, *91*, 743 (in this issue).